UNIVERSITAT POLITÈCNICA DE CATALUNYA
BARCELONATECH
Escola Superior d'Agricultura de Barcelona

MODELLING OF LIGHT DISTRIBUTION IN A CYLINDRICAL PHOTOBIOREACTOR AND STUDY OF *Ulva ohnoi* PRODUCTIVITY

Bachelor's thesis

Biosystems Engineering - EEABB

Author: Adrian Carrascosa Lopez
Tutor: Dra. Ingrid Masaló Llora
Castelldefels, June 2021

ABSTRACT

Over the last years, the study of micro and macro algae has become a matter of a major interest to the population, mainly due to their great potential. Their singular capacities, such waste water cleaners, high nutrient content, fast growth rates, or their inclusion to Integrated Multi-Trophic Aquaculture (IMTA) make them a clue pilar for future sustainable societies.

Although their promising potential, the truth is that the scientific community still has a lot to learn from them. One of the most recurrent problems in what industrial production is concerned, is knowing the exactly quantity of biomass in a specific moment inside a tank. The traditional method to evaluate their growth rates, based on drying and weighting all the biomass in the tanks, is time-consuming, and non-viable at industrial level.

The main objective of this work is the computational modelling of the light distribution inside a cylindrical photobioreactor illuminated by LEDs. By means of the proposed model, we can approach the amount of the macroalgae *Ulva ohnoi* Hiraoka & Shimada just knowing the amount of light reaching the centre, saving time and effort in regard of the traditional method.

Some studies of the *Ulva ohnoi* growth rates have been carried out varying LEDs configuration and nitrates/phosphates concentration, while measuring the chlorophyll content in the seaweed at the beginning and at the end of the experiments. As a verification of the proposed model, its efficiency was proved changing the algae density inside the reactor using the light configuration implemented in the growth studies.

The model approximations of the biomass content resulted very close to the real values in both LEDs disposition tested. The growth rates followed a decreasing tendency, and although the highest SGR was obtained with the highest light availability (0.106 day^{-1}), the nutrients availability were more significant to the algae growth.

Key words: *Ulva ohnoi*, aquaculture, photobioreactor, Lambert-Beer law

RESUM

En els últims anys, el món de les micro i macro algues s'ha convertit en un tema de gran interès per la població, principalment degut al seu potencial de cara al futur. Les seves singulars capacitats com la neteja d'aigües brutes, el seu contingut de nutrients, el seu ràpid creixement, o la seva inclusió a sistemes d'Aqüicultura Multi-Tròfica Integrada (IMTA), la converteixen en un dels elements claus per a la sostenibilitat de futures societats.

Tot i el seu gran potencial, el cert és que a la comunitat científica encara ens queda molt per estudiar i aprendre d'elles. Un dels problemes més recurrents en quant a la producció industrial de macro algues és saber la quantitat exacte de biomassa en un moment determinat a un tanc. El mètode tradicional per avaluar les taxes de creixement, basat en assecar i pesar tota la biomassa, resulta costós i inviable a escala industrial.

L'objectiu principal del present treball és la modelització computacional de la distribució de llum dins d'un fotobiorreactor circular il·luminat per LEDs. Mitjançant el model proposat, podem aproximar el contingut de la macro alga *Ulva ohnoi* Hiraoka & Shimada sabent únicament la quantitat de llum que hi arriba a l'interior, estalviant temps i esforç respecte el mètode tradicional.

Diversos estudis sobre les taxes de creixement de *Ulva ohnoi* s'han dut a terme variant la configuració de LEDs i les concentracions de nitrats/fosfats, tot i mesurant el contingut de clorofil·la a l'alga al principi i al final dels experiments. Per a verificar el model proposat, la seva eficiència ha estat provada canviant les densitats d'alga a l'interior del reactor i utilitzant les configuracions lumíniques implementades als estudis de creixement.

Les aproximacions del contingut de biomassa per part del model van resultar molt properes als valors reals a les dos configuracions de LEDs provades. Les taxes de creixement van seguir una tendència decreixent, i tot i que es va obtenir el màxim SGR amb la màxima disponibilitat de llum (0.106 dia^{-1}), la disponibilitat de nutrients va resultar ser més significativa pel creixement de l'alga.

Paraules clau: *Ulva ohnoi*, aqüicultura, fotobiorreactor, llei de Lambert-Beer

RESUMEN

En los últimos años, el mundo de las micro y macro algas se ha convertido en un tema de gran interés para la población, debido principalmente a su potencial en vistas al futuro. Sus singulares capacidades como la limpieza de aguas sucias, su contenido de nutrientes, su rápido crecimiento, o su inclusión en sistemas de Acuicultura Multi-Trófica Integrada (IMTA), las convierten en uno de los elementos claves para la sostenibilidad de futuras sociedades.

A pesar de su gran potencial, lo cierto es que a la comunidad científica aún nos queda mucho por estudiar y aprender sobre ellas. Uno de los problemas más recurrentes en cuanto a la producción industrial de macro algas es el de saber la cantidad exacta de biomasa presente en un determinado momento en un tanque. El método tradicional para evaluar las tasas de crecimiento, basado en el secado y pesaje de toda la biomasa, resulta costoso e inviable a escala industrial.

El objetivo principal del presente trabajo se centra en la modelización computacional de la distribución de la luz en un fotobiorreactor iluminado por LEDs. Mediante el modelo propuesto, podemos aproximar el contenido de la macroalga *Ulva ohnoi* Hiraoka & Shimada sabiendo únicamente la cantidad de luz que llega al interior, ahorrando tiempo y esfuerzo respecto el método tradicional.

Se han llevado a cabo diversos estudios sobre las tasas de crecimiento de *Ulva ohnoi* variando la configuración de LEDs i las concentraciones de nitratos/fosfatos, determinando el contenido de clorofila del alga al principio y al final de los experimentos. Para verificar el modelo propuesto, se ha probado su eficiencia cambiando la densidad de alga en el reactor utilizando las configuraciones lumínicas implementadas en los estudios de crecimiento.

Las aproximaciones del contenido de biomasa por parte del modelo resultaron muy próximas a los valores reales en las dos disposiciones de LEDs probadas. Las tasas de crecimiento siguieron una tendencia decreciente, y aunque el mayor SGR se obtuvo con la máxima disponibilidad de luz (0.106 dia^{-1}), la disponibilidad de nutrientes resultó ser más significativa para el crecimiento del alga.

Palabras clave: *Ulva ohnoi*, acuicultura, fotobiorreactor, ley de Lambert-Beer

Content

LIST OF FIGURES

LIST OF TABLES

SYMBOLS AND ABBREVIATIONS

I = photon irradiance in a given point (µmol photons m^{-2} s^{-1})

I_0 = incident photon irradiance to the water surface (µmol photons m^{-2} s^{-1})

K' = light attenuation constant (m^{-1})

Kw = water light extinction coefficient (m^{-1})

Kx = seaweed light extinction coefficient (m^2 g^{-1})

X = biomass per unit volume (g m^{-3})

z = distance from the wall (m)

R = PBR radius (m)

GF = Geometric Factor (m^{-1})

α = Ever's absorption coefficient (m^2 g^{-1})

θ = given angle respect ordinates (degrees º)

i = rows of Matlab matrix

j = columns of Matlab matrix

A = amplitude of sinusoidal PAR(θ) function

B = centre of sinusoidal PAR(θ) function

w = angular frequency

Φ = phase

W_f: Final weight (g)

W_0: Initial weight (g)

t = Time (days)

IMTA: Integrated Multi-Trophic Aquaculture

RAS: Recirculating Aquaculture System

PBR: Photobioreactor

PAR: Photosynthetic Active Radiation

LED: Light Emitting Diode

TAN: Total Ammonium Nitrogen

SGR: Specific Growth Rate

CCI: Chlorophyll Content Index

1. INTRODUCTION

This research project has been carried out in the facilities of the AQUAL-SPAq research group of the Polytechnic University of Catalonia (UPC), located at the Barcelona School of Agri-Food and Biosystems Engineering (EEABB) in Castelldefels, Barcelona.

1.1. Introduction to photo-autotrophic organisms

Nowadays, algae are one of the most studied organisms by the scientific community. Thanks to their variety of singular capacities, thousands of studies have been carried out in very different disciplines, such their implementation on water treatment, their role in the agri-food industry or even as a promising source of biofuel.

1.1.1. Microalgae

Microalgae are at the bottom level of the marine trophic web. They are capable of producing oxygen by doing the photosynthesis, indeed they are able to use the greenhouse gases to grow in a photo autotrophically way (obtaining energy from light, and nutrients from inorganic matter, concretely CO_2). Due to those important and singular abilities, they have been studied for years, being cultured in multiple types of photobioreactors: closed, opened, tubular, flat…

Fig 1: Three pictures of different shapes of microalgae: a) filamentous *Anabaena* spp., b) colony of *Scenedesmus* spp. and c) unicellular *Closterium* spp. (Promdaen et al., 2014)

Since our specie of interest is not microalgae, we will not deepen in their properties. However, as they share a lot of characteristics with macro algae, there will be many similarities regarding their cultivation method, their nutritional requirements or even their growth performance in a photobioreactor.

1.1.2. Macroalgae

Macroalgae are traditionally used in human and animal nutrition, mainly due to their high protein and fibre content. Furthermore, some of them have many therapeutical applications like weight control, antioxidant or antitumor activities, which make them a very valuable source of research (Patarra et al., 2011). Macroalgae are classified into three major groups:

Chlorophyta or 'Green Algae' cells contain chlorophyll pigments that gives their characteristic colour. We can find them either in sea, river or lakes, and there are more than 6000 species, one of which is *Ulva ohnoi*, the specie studied in the present work.

Between 1500 and 2000 different species of the *Phaephyceae* class or 'Brown Algae' are known worldwide. It contains the largest sizes of algae, like *Laminaria* or simply 'kelp', which can reach the 60 meters length, creating underwater sea forests and providing refuge for all kind of organisms. Their colour varies with the proportion of two pigments: one brown (fucoxanthin) and another one green (chlorophyll). Some of these seaweeds have an important role in oriental societies diets, like Nori or Kombu (Britannica, 2018).

Finally, *Rhodophyta* or 'Red Algae' comprises over 10000 described species. The fact that Chlorophyll *a* is the only chlorophyll, combined with the high production of the polysaccharide phycobilin, makes the red colour predominance instead of green (Seo et al., 2010; Lin & Lin, 2011; Barsanti, Laura & Gualtieri, 2010).

Fig 2: a) *Ulva ohnoi* (SPAq-lab UPC), b) red algae *Asparagopsis taxiformis* (Azzopardi, 2019), c) brown algae *Laminariales* spp. or 'Kelp' (Martinez, 2020)

1.2. IMTA Systems

Nowadays, aquaculture industry is one of the main economical pillars in some countries, and its sustainability a political and public concern. However, aquaculture farms can have a negative impact in marine environment due to the release of excess nutrient from faecal matter, or even from uneaten feed. With the expected growth in global population and consequently in food production, solutions are needed to reduce such load of nutrients in this sector (Ellis & Tiller, 2019).

Integrated Multi-Trophic Aquaculture (IMTA) offers many advantages to fight against these environmental problems caused by traditional aquaculture farms. IMTA principles are based on nutrient recycling, growing species from different trophic levels (fish, shellfish, seaweeds…) in a single system, allowing to feed one with the waste of the other, while delivering economic benefits and public support (Rosa et al., 2020).

Organic and inorganic extractive species, like shellfish and seaweeds respectively, play an important role in IMTA. Their capacities to reduce the nutrient loading by consuming the particulate organic matter and dissolved inorganic nutrients creates a balanced, circular and environmentally friendly system, adding value for culturing biomass in proximity with each other.

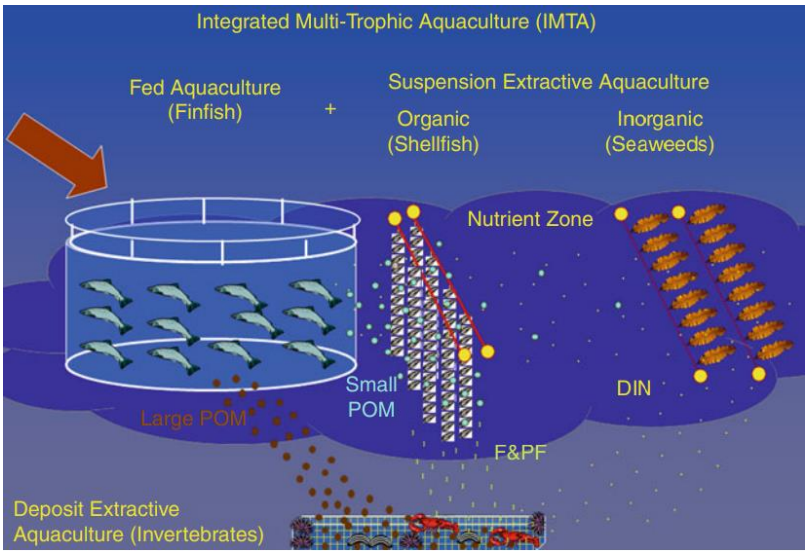

Fig 3: Conceptual diagram of IMTA in open waters, with combination of fed aquaculture (Finfish) with suspension of extractive species. POM (Particulate Organic Matter), DIN (Dissolved Inorganic Matter) and F&PF (Feces and Pseudo Feces) (Chopin, 2013)

As we can see in **Figure 3**, IMTA systems can be placed on open waters (sea or bay), and also on land. Among Integrated Multi-Trophic Aquaculture techniques, the integration of fish and macroalgae cultures in Recirculating Aquaculture Systems (IMTA-RAS) is currently on of the most promising lines of action, achieving diversification and sustainability in aquaculture activities. The main advantages of these systems are the improvement of waste water management, the optimization of feed inputs, and the minimization of energy resources (Waller et al., 2015).

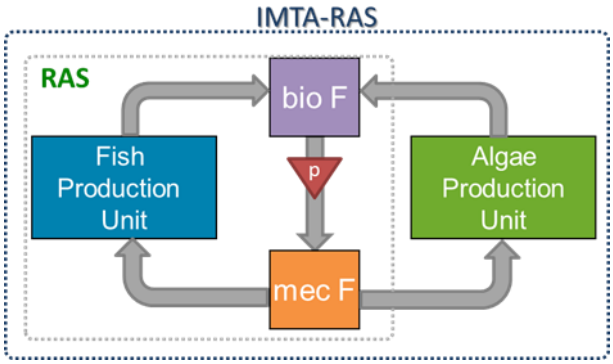

Fig 4: Basic scheme of IMTA-RAS system

In an IMTA-RAS system, water outcoming from the fish pass to a mechanical filter (mec F) and to a biofilter (bio F). TAN from fish excretions (Total Ammonia Nitrogen, NH_4 + NH_3) is first converted into nitrites (NO_2^-) by *Nitrosomonas* sp. and secondly into nitrates (NO_3^-) by *Nitrobacter* sp., which is less toxic for fish than ammonia.

As an inorganic extractive organism, seaweed is the responsible of cleaning the 'dirty' water coming from the fish tank. Their functions are not limited to take the dissolved inorganic nutrients as ammonium and phosphate. Thanks to photosynthetic action, they are able to oxygenate the water which is returned to fish tanks, until such a point that seaweeds are considered the bioremediators in aquaculture (Rosa et al., 2020).

1.3. Ulva ohnoi

This chapter puts in context the main characteristics and properties of *Ulva ohnoi*, which as it was said before, is one of the main pillars of our IMTA systems, and the main focus on the research plan.

1.3.1. Description

Ulva ohnoi Hiraoka & Simada was firstly described in the southern and western of Japan, country from which it is considered endogenous. It belongs to the phylum Chlorophyta, to the class Chlorophyceae (green algae) and to the order *Ulvales*. *Ulva* spp. are essentially marine green algae generally found on rocky shores and even attached to rocks or stones. It can also be found in brackish waters or estuaries, and there are more than 125 species of *Ulva* taxonomically accepted (Hiraoka et al., 2004).

Marked seasonal variations can change the morphology of this algae: whereas a young organism is dark green and soft to the touch, the older ones become light green and their surface slimy (Baweja, 2016). It approximately has a thickness of 30-55 µm and a very irregular growth in surface, so the algae can easily grow until 50cm.

Ulva provides many services for aquaculture and the food industry. Due to its high photosynthetic and growth rates (explained during the next chapters), it is often used as a biofilter in IMTA systems, reducing the organic matter from fish effluents. Moreover, thanks to its high carbohydrate content, which can reach the 40% of its dry weight, *Ulva* is often studied as a potential source for bioethanol production (Grimes et al., 2018).

1.3.2. Parameters affecting algae growth

As it was said before, the growth of any living organism will be strongly related with the conditions in which it is grown. In *Ulva* cultures, the main parameters affecting their growth must be controlled. These parameters are:

Supply of light energy

For phototrophic organisms, which take photons as energy source, light can be a very relevant parameter for their correct development. However, it can also be a limiting factor if we do not adequate it for each studied specie (Suh & Lee, 2003).

When selecting a light source, we have to consider the quality and also the quantity of light. Whereas the first one is related with the absorption spectrum (which for photosynthetically active pigments must be between 400 and 700nm), the second one refers to the light intensity.

Carbon dioxide and oxygen removal

In photo autotrophically organisms, CO_2 (and subsequently bicarbonate once has been dissolved into water) is the main carbon source for growing cells. Due to the poor exchange between air and water (0.03% according to (Suh & Lee, 2003)), in cultured algae systems, it is usually needed additional CO_2 for the correct algae growth.

As a product of the photosynthesis, oxygen (or particularly a bad oxygen removal) can be a limiting factor too, so it can inhibit algal growth. An increase in the bioreactor turbulence to have more contact between air and water might be the main solution for this problem, creating a correct exchange of nutrients and gases between algae and water.

Nutrients

Nutrient availability is also a relevant factor for the correct algae growth. The essential nutrients, also called macronutrients, are nitrogen, phosphorous, sulphur, calcium, magnesium, sodium, potassium and chlorine (Suh & Lee, 2003). Nutrients needed in less quantities, called micronutrients, include iron, boron, manganese, copper… if there is a lack of those nutrients, algae can secrete autoinhibitory compounds, so the growth may be consequently and negatively affected.

pH

Other abiotic factors like temperature and pH have also a strong relevance in each algae culture. Especially pH has a key role in the assimilation of some molecules needed for the correct algae growth. **Fig.5** shows the main interactions between algae and the environment:

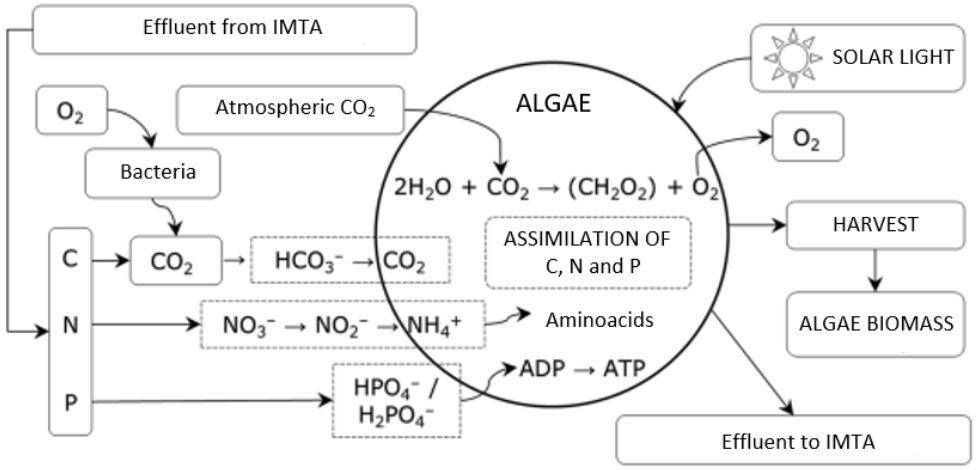

Fig 5: Environmental factors for algae (Beltrán-Rocha et al., 2017)).

During the photosynthesis, algae assimilates inorganic carbon from CO_2 coming from atmosphere or bicarbonate coming from the effluents. However, high concentrations of CO_2 produce an acidification of the medium, increasing the concentration of carbonate (CO_3^-, inaccessible for algae) instead of bi-carbonate (HCO_3^-), reducing algae growth and affecting negatively the culture.

1.4. Photobioreactors

Bioreactors are manufactured devices in which biological or chemical processes are carried out in order to obtain some kind of product, such secondary metabolites, enzymes or proteins, or to accomplish some kind of process, such water treatment or biocatalysis. In our case, bioreactors are used for macro-algae production and water treatment coming from IMTA.

There are many ways to classify bioreactors, such by their operational conditions, their geometry or by their mixing mode. We talk about 'Photobioreactors' when light source is used to cultivate phototrophic organisms in a controlled environment (Erickson, 2011). In land-based systems, algae can be produced in Open ponds or in closed photobioreactor systems. Their respective advantages and limitations are explained in the next table:

Table 1: Advantages and disadvantages of open and closed photobioreactors (Rajendran, 2016)

Parameters	Open ponds (raceway ponds)	Closed systems (PBR)
Contamination risk	High	Low
Water losses	High	Low
CO_2 losses	High	Almost none
Reproducibility of production	Variant but consistent over time	Possible within certain tolerances
Process control	Complicated	Less complicated
Standardization	Difficult	Possible
Weather dependence	High	Less because protected
Maintenance	Easy	Difficult
Construction costs	Low	High
Biomass concentrations at harvesting	Low	High
Overheating problems	Low	High
Super dissolved oxygen concentrations	Low	High

While ponds present lower construction and maintenance costs, closed systems are characterized for having a better control during the culture development and higher biomass production rates.

Another way of classifying bioreactors is by their operational methodology. We can distinguish between batch, fed-batch and continuous. Whereas in batch models there are no inputs neither outputs from the system in a continuous way, in fed-batch liquid media is fed to the bioreactor without any outflow. Otherwise, continuous models are characterized by having continuous inflows and outflows of substrate and product, respectively. Ponds are a clear example of this last kind of systems (Erickson, 2011).

1.5. Light availability in the PBR

As it was explained before, light is one of the most limiting factors for any kind of photoautotrophic organism. Having the adequate light availability will determine the growth and health of our algae cultures. In this chapter, we will see the nature of light and how we can study it depending on the geometry of the PBR and light source.

1.5.1. Light nature

Light is mainly electromagnetic radiation transmitted by transparent mediums. Our radiation of interest is between 400 and 700 nm, and it is called Photosynthetic Active Radiation (from now on PAR). Shorter radiations below 350 nm can damage the photosynthetic cells (Rajendran, 2016) due to its high energy. Indeed, wavelengths longer than 700 nm have not enough energy to initiate the photosynthetic process.

Irradiance *I* is the PAR radiation providing from all directions, and its units are quantity of radiation per unit area and time. We can also study it with energetic units (for example W/m^2) or quantum units, which in our case is µmol of photons m^{-2} s^{-1}. There are two kind of sensors to measure the irradiance: 4π and 2π; while the first one measures irradiance from all directions, the second one only takes measures from one hemisphere.

1.5.1. Influence of the geometry

In order to study the irradiance along the section of a PBR with transparent walls applying the Lambert-Beer Law, we will first have to study their geometry and its influence on the light transmission model.

In the present study, a cylindrical photobioreactor is illuminated with LEDs disposed all along the surface. Those LED's have a helix shape, so we will have to take into account this shape when modifying the model and consider the extinction radially.

In what flow or light transmission model is concerned, we can find three different ways of how light arrives at each point:

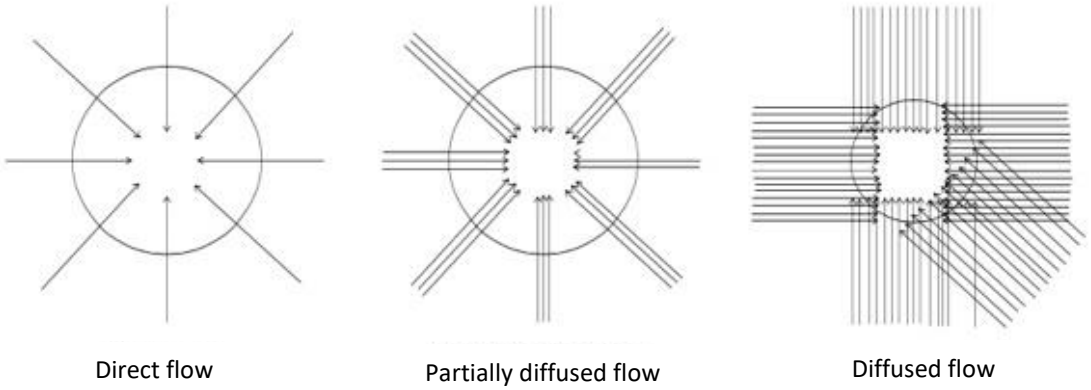

Fig 6: Some models of light flow. Source *(Sevilla, 2014)*

In the direct flow, photons reach one point from only one direction. This happens for example with solar rays because they travel in parallel. In the diffuse flow, photons reach one point from all spatial directions. In our case, irradiance would come from each point of the perimeter of the circumference.

1.5.2. Lambert-Beer Law

One of the most studied equations for the light distribution is the Lambert-Beer Law, which describes the photon irradiance at a certain depth I(z):

$$I(z) = I_0 * \exp(-K' * z) \quad \textbf{Eq. 1}$$

According to this model, we assume an external light source I_0 irradiating the water surface. The incident photon irradiance is attenuated through the water column by absorption and scattering, decreasing exponentially with depth *z* and with the light attenuation constant *K'* (m^{-1}).

We can find an extensive bibliography related to this model, and many modifications have been suggested in order to adapt the Lambert-Beer Law (Katsuda et al., 2000).

In a macroalgae tank, *K'* is determined by the water extinction coefficient and by the seaweed biomass per unit of volume. Finally, we get the following equation:

$$I(z) = I_0 * \exp(-(kw + kx * X) * z) \quad \textbf{Eq. 2}$$

Where:

- *I(z)* = photon irradiance at depth *z* (µmol photons m^{-2} s^{-1})
- I_0 = photon irradiance at the water surface (µmol photons m^{-2} s^{-1})
- *Kw* = water light extinction coefficient (m^{-1})
- *Kx* = seaweed light extinction coefficient (m^2 g^{-1})
- *X* = biomass per unit volume (g m^{-3})
- *z* = distance from the wall (m)

Finally, applying this formula, we are accepting the next three assumptions (Acién Fernández et al., 1997):

a) The direction of the incident radiation does not change as it crosses through the culture, so we are talking about direct flow
b) The radiation is monochromatic
c) Scattering effect due to solid particles is negligible compared to the absorption effect

1.5.2.1. Evers Model

In 1991, E. G. Evers modelled how growth of phototrophic organisms in continuous cultures were affected by light limitations. In his study, Evers proposed that mutual shading of cell could not be neglected if the amount of biomass inside the tank was enough to influence on the light distribution inside the vessel. Since cylindrical PBR illuminated from all sides was the most commonly used way to cultivate phototrophic organisms, he focused his work on this kind of vessel (Evers, 1990).

He was firstly based on Lambert-Beer law, which as it was explained before, light attenuation is caused by cellular absorption. However, unlike the proposed model explained in the previous chapter, light paths obey a diffused flow, so photons reaching one point of the section come from all spatial directions. Such directions will be restricted to one plane (Sevilla, 2014).

Looking to **Figure 6** *c) Diffused flow*, light comes from 5 directions. If it came from infinite directions, from every direction θ we need a differential $dI = (I_0/2\pi)\, d\theta$, or $dI = (I_0/\pi)\, d\theta$ if it came only from one hemisphere. Applying such concepts, Evers proposed the following mathematical model in which light from all directions $\{0 \le \theta \le 2\pi\}$ has to be taken into account. For reasons of symmetry, it is enough to consider $\{0 \le \theta \le \pi\}$:

$$\boldsymbol{I(z,X) = \frac{1}{\pi}\int_0^{\pi} I(\theta,z,X)\,d\theta}$$

$$\boldsymbol{= \frac{I_0}{\pi}\int_0^{\pi} \exp\left\{-\alpha * X * \left[(R-z)\cos\theta + (R^2-(R-z)^2\sin^2\theta)^{0.5}\right]\right\} d\theta} \quad \textbf{Eq. 3}$$

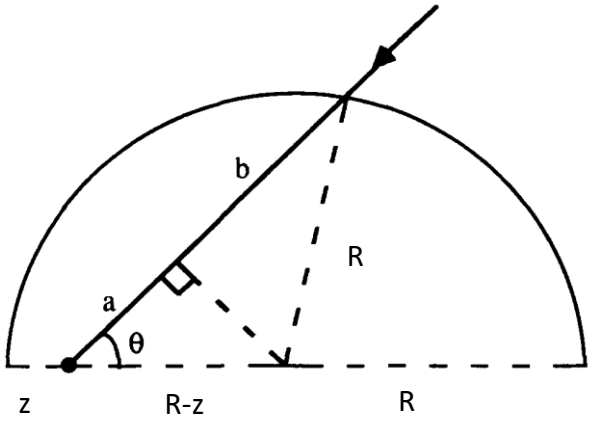

Fig 7: Evers' schematic representation of one half of a cross section through a cylindrical PBR (***ab***, light path; ***R***, cylinder radius; ***z***, distance from the vessel surface; **θ**, angle of light path with line through the centre) Adapted from (Evers, 1990)

2. OBJECTIVES

The main objective of this work is to create a computational model to predict the amount of biomass just knowing the light PAR at the centre of the PBR. Some others specific targets are:

- Modelling the light distribution inside the PBR applying the Lambert-Beer law
- Analyse *Ulva ohnoi* growth rates within different culture conditions (light and nutrients)

For both goals, a cylindrical photobioreactor illuminated with LEDs will be used, studying two different light configurations.

3. MATERIALS AND METHODS

3.1. IMTA facilities

The work was carried out in SPAq-UPC research group laboratory located in the EEABB Campus (Castelldefels). The laboratory includes an IMTA-RAS system with soles (*Solea senegalensis*) and *Ulva ohnoi*.

14 soles were placed in one tank (T2 in **Fig.8**) of approximately 0.9 m^2, being 14 the current individuals. Algae are distributed in five tanks, three of them are cylindrical (R1, R2 and R2) with a surface of 0.32 m^2 and a volume of 90 litres, and two are semi cylindric tanks with rectangular surface of 0.64 m^2 (NA1 and NA2) and a volume of 172 litres. Both types of tanks are mixed with aeration from the bottom.

The effluents of the fish tank were passed through a mechanical filter and drained to a buffer tank of 0.6 m^2 (EXP tank in **Fig.8**) where the biofilter was placed; water was recirculated from the buffer tank to the fish tank, while a small volume of the buffer tank water was delivered to the algae tank with a peristaltic pump. pH is controlled using chlorohydric acid, which is added to the buffer tank also with a peristaltic pump. We can see a basic scheme of the facilities in **Fig.8**:

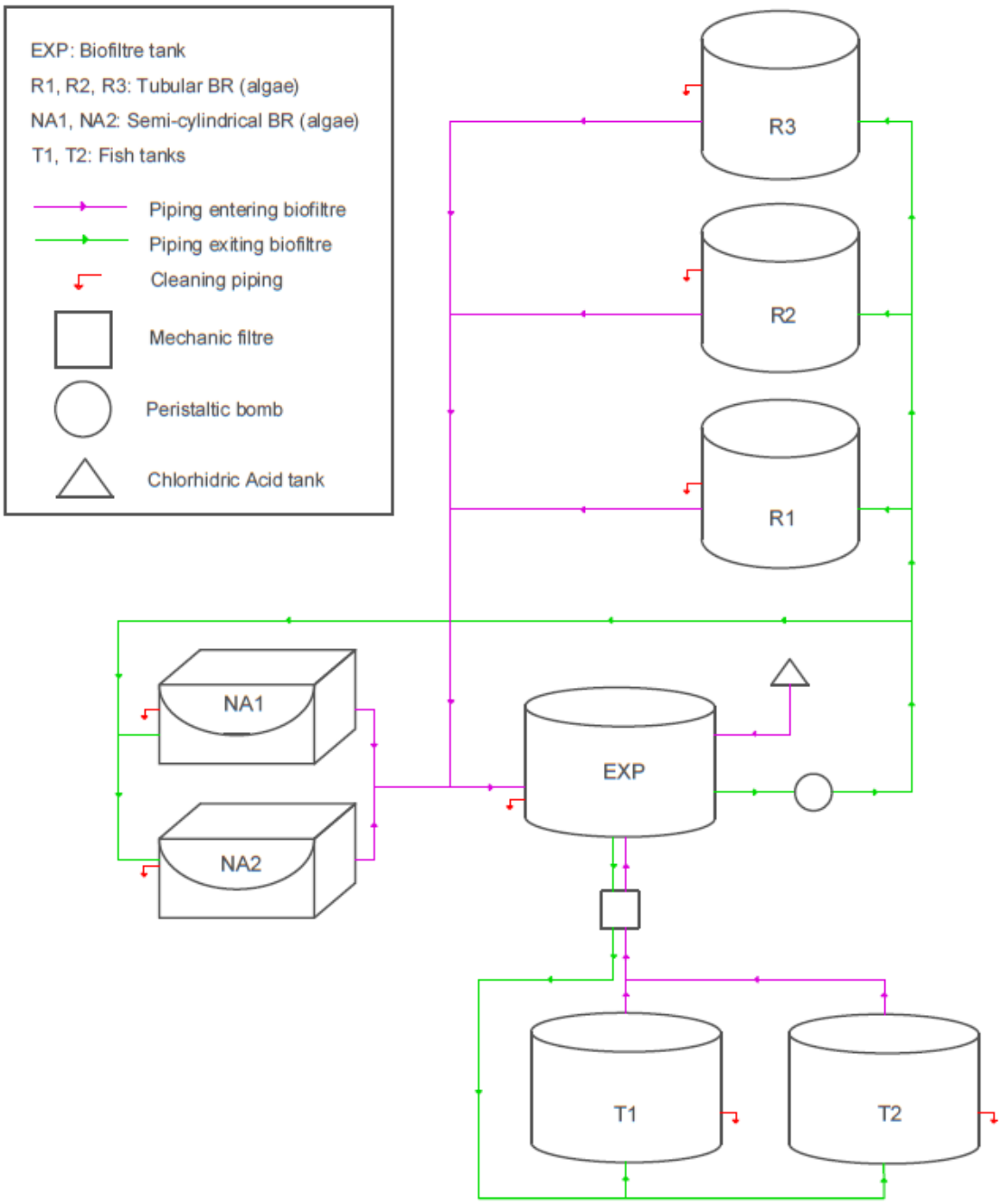

Fig 8: Basic scheme of the IMTA facilities in the SPAq – UPC research lab

3.2. Photobioreactor used

Both experiments (algae growth and modelling of the light irradiance) were carried out in a tubular photobioreactor 45 cm of height, 7 cm of radius and approximately a volume of 4 litres. The light source were LEDs disposed on the walls of the reactor, creating a spiral shape all along the vertical axis. Air coming from the bottom of the PBR mixes the biomass, creating a vertical movement of the seaweed (**Fig.9**).

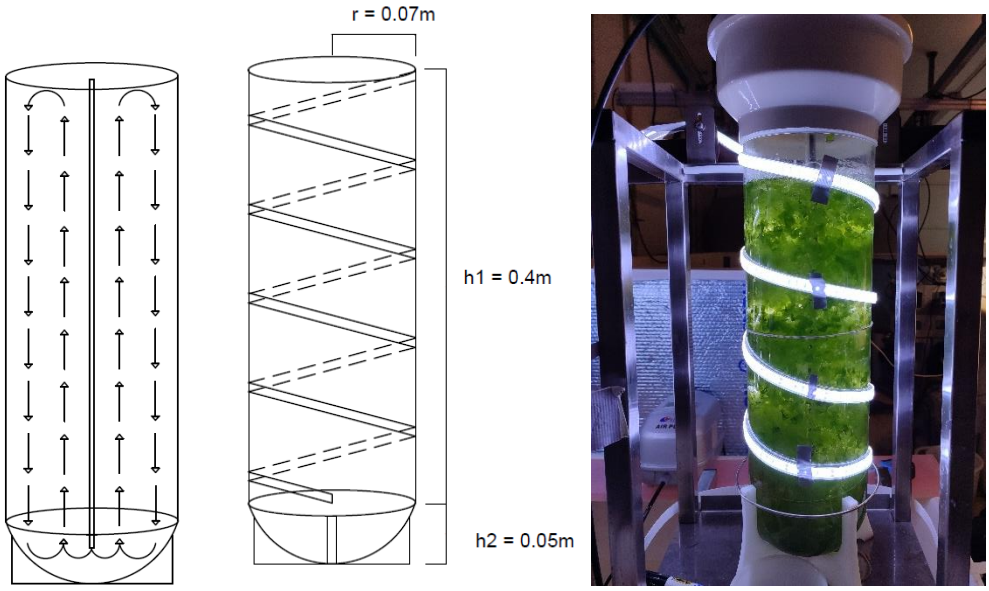

Fig 9: On the left, scheme of mixing distribution. On the middle, LEDs disposition. On the right, photo of the photobioreactor used (own source)

The photobioreactor used during the experiments were external from the IMTA systems, and the experiments were carried out in batch conditions: water was only added when volume decreased as a consequence of evaporation or because water was withdrawal to analyse.

3.3. Parameters controlled during the experiments

Temperature, Oxygen and pH

Temperature (ºC), Oxygen Concentration (mg/l) and Saturation (%) in the algae tanks were measured with a probe (Handy Polaris Oxyguard). Its easy management and simple data screen make it a useful tool to this kind of measurements. On the same way, pH was measured also with a probe (Handy pH Oxyguard).

Salinity and Alkalinity

Salinity (g/l) was measured using a digital Seawater Refractometer (Hanna). Alkalinity was determined by acid-base titration against sulphuric acid with cromogen.

Nitrates, Phosphates and TAN

The methodology to determine the nitrates and phosphates concentrations in the algae tank was using a spectrophotometer according to (APHA 1992) and (Frasshoff et.al., 1999). Detailed explanation of each method is described in APPENDIXES A and B respectively. The Total Ammonium Nitrogen (TAN) of the water was measured with a photometer of EcoSense 9500, YSI (**Figure 10 c)** .

Chlorophyl content

The content of the chlorophyll was measured with a MC-100 Chlorophyll Concentration Meter. This optical meter outputs the measure of Chlorophyll Content Index (CCI), which is calculated by the radiation transmittance from two wavelengths (653 and 931 nm). If we want to know the total concentration of chlorophyll (including both ***a*** and ***b*** chlorophylls) we followed the equation proposed in (Masaló & Oca, 2020):

$$y = 66.529x - 58.185 \quad \textbf{Eq 4}$$
$$R^2 = 0.935$$

y representing the Total Chlorophyll (µmol m^{-2}) and **x** the CCI obtained with the probe.

PAR

Photosynthetic Active Radiation was measured with a Universal Light Meter & Data Logger sensor ULM – 500 Walz; the light meter includes a 4π sensor, which is a spherical sensor with an irradiance response coming from all directions.

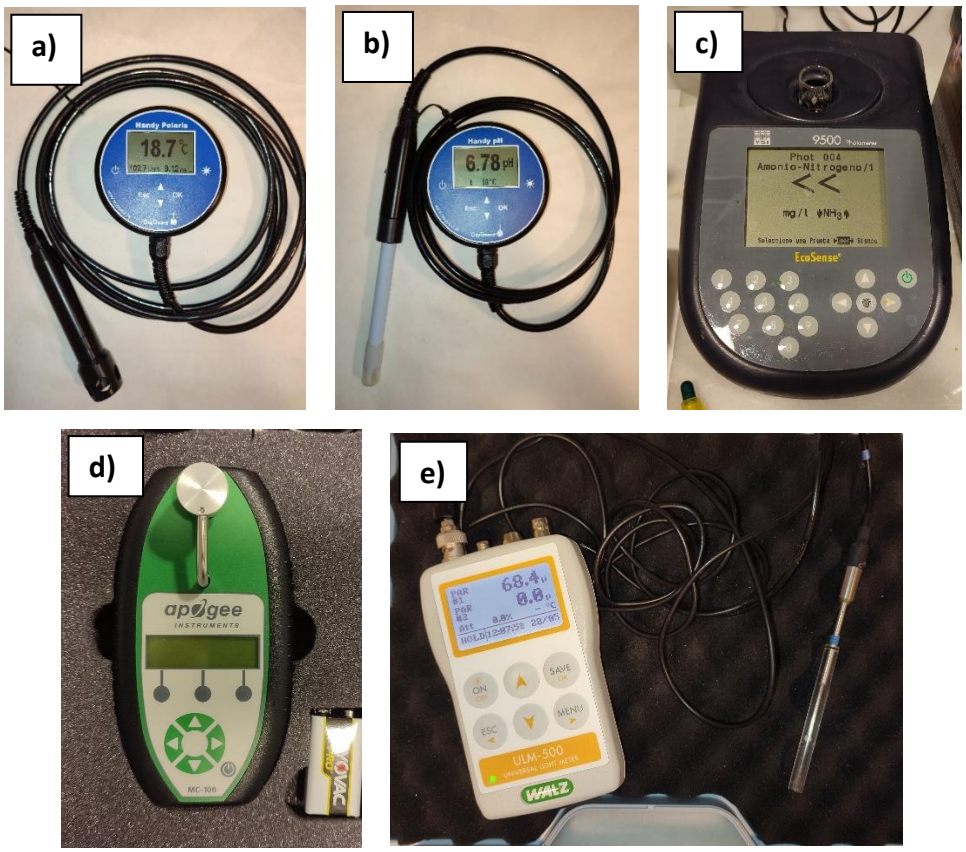

Fig 10: Photos of a) Handy Polaris Oxyguard, b) pH Oxyguard, c) EcoSense 9500, d) MC-100 CCM and e) ULM – 500 Light meter

3.4. Culture conditions

The starting biomass in the cultures was always taken from the same IMTA tank. The selection procedure was simple: the biggest and healthiest fronds of algae from the tank R3 were taken, centrifuged and dried with lab paper. Chlorophyll content was determined, and finally the fronds were cut into smaller fragments by a cut cookware. Such tool helped us to obtain fragments with approximately the same surface (**Fig 11**).

The measure or surface was taken using the program ImageJ. The aim of this procedure was to ensure the best homogeneity inside the bioreactor, so every algae fragment had the same initial surface and the same chlorophyll content (almost all fragments came from the same algae). Using such tool, we got fragments with an approximate surface of 0.35 cm^2 per unit of algae with a standard deviation of 0.15 (n = 100).

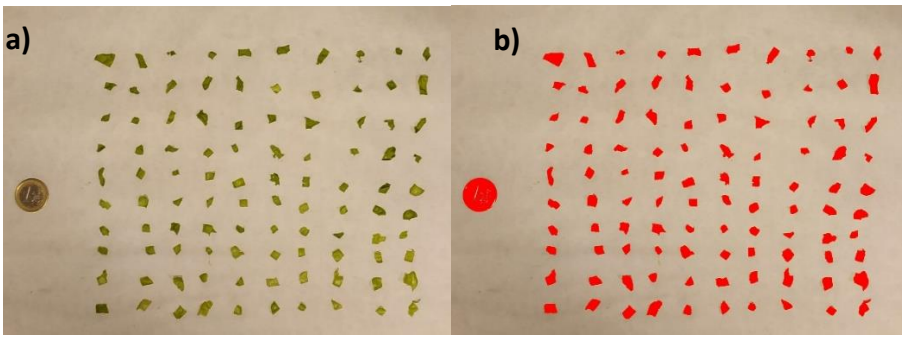

Fig 11: ImageJ processing. Photos regarding the first culture. a) before and b) after image processing

Once measured the surface, 7 g of *Ulva ohnoi* were weight and introduced to the PBR as the starting biomass. The initial culture medium was always water coming from the EXP tank of IMTA. During the experiments, some water had to be refilled in order to maintain always the same volume; volume decrease was consequence of evaporation and/or withdrawn to analyse nitrates, phosphates and TAN.

Three consecutives experiments were carried out during the research time. The main differences came with the light source and the nutrient refill:

- **First culture:** from 26/02 to 19/03. LEDs pitch of 10 cm. Water refilling when needed: EXP tank (water with nutrients).
- **Second culture:** from 07/04 to 28/04. LEDs pitch of 10 cm. Water refilling when needed: saltwater (water without nutrients).

- **Third culture:** from 05/05 to 26/05. LEDs pitch of 6 cm. Water refilling when needed: mixing of saltwater and EXP tank

The measures of all the factors described in the previous chapter were done on weekdays at about 8-9 am. Lights were OFF in that time, and they turned on at 10 am until 10 pm, having a light cycle of 12:12. Before 10 am it is considered that the bioreactor has the lowest oxygen concentration, since algae have been doing respiration all night long. The conditions and time-lines of each culture are described in the following table:

Table 2: Mean of every measure ± standard deviation of each culture

	First culture (26/02-19/03)	Second culture (07/04-28/04)	Third culture (05/05-26/05)
T_{room} (ºC)	16.9 ± 0.2	19.1 ± 1.0	20 ± 1.2
T_{PBR} (ºC)	15.5 ± 0.5	17.1 ± 1.0	18.8 ± 1.5
O_2 (mg/l)	8.2 ± 0.3	7.93 ± 0.3	7.6 ± 0.1
Sat (%)	96.6 ± 2.8	96.9 ± 2.8	95.9 ± 1.8
pH	8.7 ± 0.3	8.3 ± 0.2	8.8 ± 0.2
Salinity (g/l)	38.0 ± 2.6	35.4 ± 2.7	35 ± 1.8
Initial fresh weight (g)	7	7	7
LEDs distance (cm)	10	10	6
Water refilling	From Biofilter IMTA	Saltwater	Mix

Ulva ohnoi growth performance was parametrized measuring the fresh weight once per week and determining the Specific Growth Rate (SGR), which indicates how much has the algae grown in a determinate time (units of day^{-1}):

Where:

- W_f: Final weight (g)
- W_0: Initial weight (g)
- t = Time (days)

$$SGR = \frac{ln\left(\frac{W_f}{W_0}\right)}{t}$$

The three cultures had approximately the same length (21-23 days), and the measure of weight was taken once per week. Unless some unexpected times at the end of the experiments, nutrients concentration were also measured once per week, following the guidelines explained in chapter **3.3**.

3.5. Description of the light model proposed

3.5.1. New Lambert-Beer equation

As it was said in chapter **1.5.2**, Lambert-Beer Law **(Eq. 2)** is the most used model in light distribution in bioreactors. Thanks to its precision and good description of the light attenuation, it has been used in many studies, and some modifications have also been proposed in order to adapt the formula to the work conditions. Let's take a brief reminder of the Lambert-Beer Law:

$$I(z) = I_0 * \exp\left(-(Kw + Kx * X) * z\right) \textbf{ Eq. 2}$$

This formula describes how light irradiated from the surface is attenuated thorough the water column by the action of 1) the water and 2) the biomass. The biomass homogeneity within the bioreactor will be a clue factor when applying Lambert-Beer law, so high heterogeneity can give non-realistic measures.

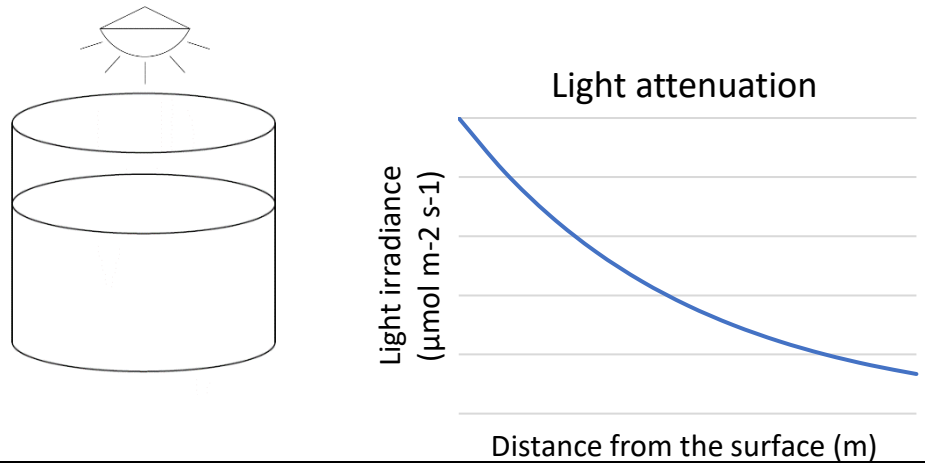

Fig 12: An example of a tubular photobioreactor illuminated from the surface (own source)

Tanks R1, R2, R3, NA1 and NA2, which have opaque walls and are illuminated from the surface, are clear examples of this kind of light attenuation described in **Fig.13**. However, the geometry of our photobioreactor and the light source differ from the last ones, having transparent walls and being illuminated from the sides, so we have to adapt Lambert-Beer Law to the new circumstances.

As we saw in chapter **3.2**, in a tubular bioreactor, light comes from the surface of the glass walls, and not from the upside of the tank, so light will be attenuated radially and not linearly (from water surface to the bottom of the tank). In addition, as LEDs are disposed in a spiral shape, I_0 will not be constant for each point of the perimeter.

In order to adapt Lambert-Beer law to these circumstances, the following model has been proposed:

$$I(z,\ \theta) = I_0(\theta) * \exp\left(-(GF(\theta) +\ Kw + Kx * X) * z\right) \quad \textbf{Eq. 5}$$

According to this radial attenuation, irradiance must be studied two-dimensionally, so with the computational program we will work using matrixes for each variable, representing every point of the PBR section. The way of referring to the position of each point can be either the common ordinates and abscises, or the angle respect ordinates and distance from the PBR wall, θ and *z* respectively.

Matrixes sizes are 101 columns and 101 rows, so for any measure of distance, a conversion factor must be applied. Working with matrixes will help us to work more efficiently, being able to combine the different parameters combining their respective matrixes.

There is a proposed new parameter in **Eq. 5**: GF(θ) or Geometric Factor. This parameter depends on each angle θ and will be the factor that determines the helix shape of the LEDs. During the next chapters we will see how we obtain this new variable and how does it affect the modelling.

3.5.2. Depth matrix

Taking a random section of the PBR, every point of such section needs a value of distance from the nearest wall, where the light source is located. From now on, this value is called depth, and in **Eq.5** is expressed as 'z', in meters.

Before creating the matrix of 'Depth', matrixes 'X' and 'Y' are obtained, which represents the coordinates of each point of the section (**Fig.13**). By trigonometry, we can find the distance from the centre, and consequently the distance from the wall. As the matrix size is 101*101 cells (in Matlab, rows are represented with *i* and columns with *j*), a conversion factor is applied to transform the obtained value into the real distance, following **Eq.6**:

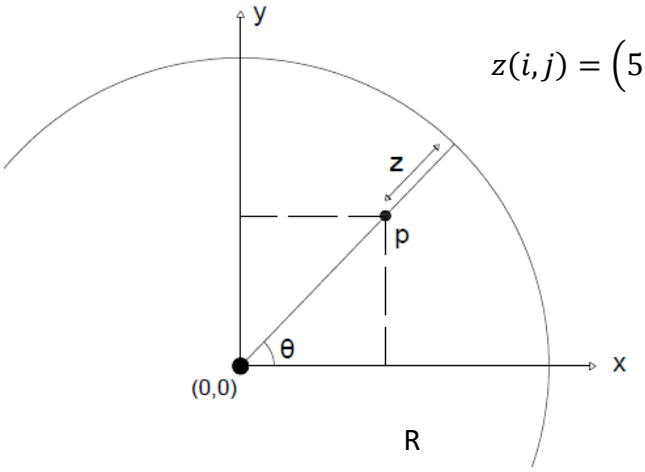

$$z(i,j) = \left(50 - \sqrt{X(i,j)^2 + Y(i,j)^2}\right) * \frac{R}{50} \quad \textbf{Eq. 6}$$

Fig 13: Depth of a random point p obtained by trigonometry. i and j represent respectively the row and the column of each cell from the matrix.

Applying **Eq. 6**, we can also delete numbers less than 0, which represent points out of the circumference. Finally, we obtain a matrix with a circular shape that will help us to interpret better the system and the PBR geometry.

3.5.3. I_0 matrix

The aim of this matrix is to give a value of I_0 to all the cells in the matrix. Starting from the surface, if we take a transversal section of the PBR and measure the light at the perimeter of the circumference (which is actually the light source I_0), we will notice that each point has a different value. This is mainly due to the shape of the LEDs disposition, projected in the next **Fig.14**.

If we measured light irradiation along the surface of the PBR in a random height, we would obtain a sinusoidal function as follows:

$$PAR(\theta) = A * \sin(w\theta + \phi) + B \quad \textbf{Eq. 7}$$

Where:

- PAR(θ): represents the Photosynthetic Active Radiation at given angle θ
- A and B: amplitude and centre, respectively
- w: angular frequency (2πf, where frequency is 1/2π, so w = 1)
- Φ: phase (π/2)

A and B are unknown values, which we will have to obtain fitting the input data with **Eq.7**. In Matlab we do not have the function 'Solver' as we have in Excel, so A and B will be obtained numerically as follows:

$$A = \frac{I_0(0º) - I_0(180º)}{2}$$

$$B = A + I_0(180º)$$

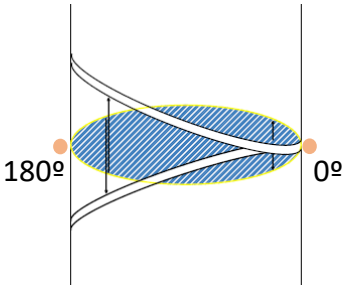

Fig 14: How the model obtains the values of Amplitude and Centre

$I_0(0º)$ represents the value of the section point in which the irradiance is higher (where actually passes the LEDs spiral) and $I_0(180º)$ represents the lower irradiance point.

3.5.4. *Kw* and *GF* Matrix

Kw is the light extinction coefficient due to the water, measured in m^{-1}. We can obtain this value from abundant bibliography (Oca et al., 2019) but we can also calculate it easily from **Eq.2** with absence of biomass inside the photobioreactor:

$$Kw = \frac{\ln\left(\frac{I(R)}{I_0}\right)}{-R} \quad \textbf{Eq. 8}$$

Nevertheless, if we measured this coefficient in our case of study, we would notice that it has a different value for each light path at given θ. Having a variable irradiance at the surface and a constant irradiance at the centre, we need some additional variable that adjust the extinction coefficient within our geometry. This new variable will be called Geometric Factor or *'GF'*, and will be defined as a matrix:

$$GF(\theta) = \frac{\ln\left(\frac{I(R,\theta)}{I_0(\theta)}\right)}{-R} - Kw \quad \textbf{Eq. 9}$$

GF matrix will be always equal, because the amount of biomass does not affect the value, so it will only change if we modify the size of the PBR or the light source shape. We can say that this matrix is clue for the adaptation of Lambert-Beer law to a spiral irradiance, and so it will be strongly related with the PBR conditions. In any case, we also need a constant *Kw* value, which will be taken from (Oca et al., 2019).

Finally, the last incognita is the seaweed extinction coefficient or *Kx*. In order to have an experimental value, some experiments have been carried out. Such experiments are described in chapter **4.2.1** and they are based on the implementation of the model varying the values of biomass and measuring light at the centre of the PBR.

4. RESULTS AND DISCUSSION

4.1. *Ulva ohnoi* growth

Three consecutive experiments were carried out varying the LEDs disposition and type of water inputs, observing how the *Ulva ohnoi* growth was affected by such factors. The respective culture conditions of each experiments are described in **Table 2**, and in this chapter, the results are presented and evaluated.

Table 3 shows a summary of the results. Although columns of weight and SGR are totally related with *Ulva ohnoi* growth performance, Nitrates and Phosphates data are strongly dependent to the type of water refilling during the experiment, and not only to the nutrient consumption from the algae:

Table 3: Summary of every experiment growth and nutrient evolution

	Week	Fresh weight (g)	SGR (day^{-1})	Nitrates (mg/l)	Phosphates (mg/l)
Culture 1 (26/03-19/03)	1	7		76.63	2.15
	2	12.519	0.083	78.13	2.09
	3	20.865	0.073	68.77	1.98
	4	28.372	0.044	72.83	1.80
Culture 2 (07/04-28/04)	1	7		74.15	1.51
	2*	16.078	0.104	66.90	0.86
	3	23.391	0.063	49.64	0.46
	4	28.447	0.028	46.64	-
Culture 3 (05/05-26-05)	1	7		59.47	0.58
	2	14.679	0.106	54.50	-
	3	21.939	0.057	50.00	-
	4	28.413	0.037	-	0.42

*second week measurement of the second experiment was 1 day later regarding the same measure of the rest of experiments

First of all, the results obtained regarding the initial and final weight of the three experiments resulted very similar among them. They all started with 7 g, and finished with approximately 28.4 g, which means a general SGR of 0.067 day^{-1}. The starting algae surface was always the same, following the guidelines described in chapter **3.4.** Surface at the end of each culture was not measured. Comparing the data obtained from **Table 3**, we obtain the following plot:

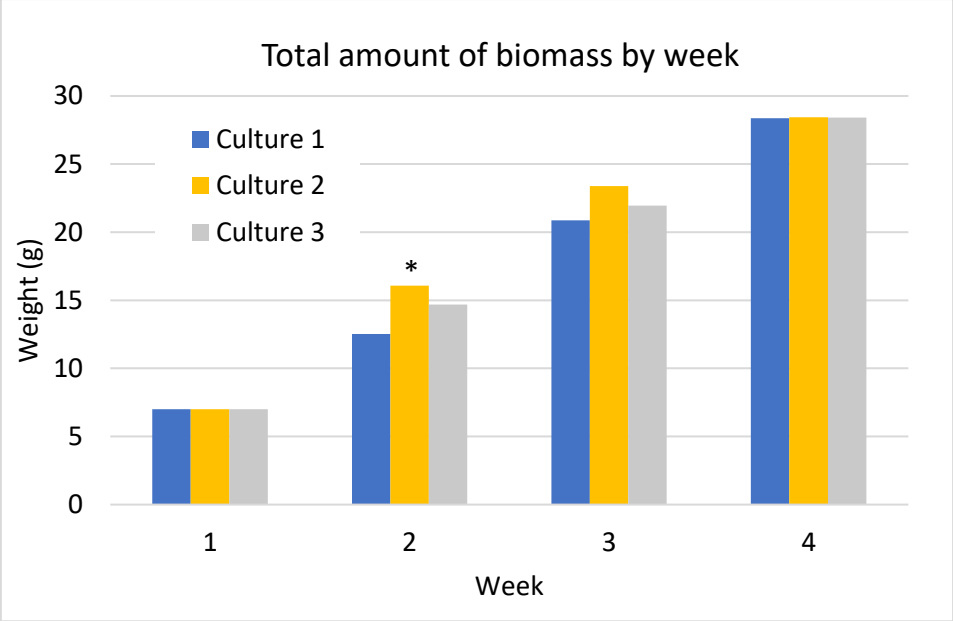

Fig 15: Evolution of total wet biomass inside the PBR for each experiment (* measure 1 day later)

During the first part of the experiments, the lower Specific Growth Rate is observed during the first culture, which although having nutrient excess, the temperature of the PBR is not the appropriate for the correct growth of *Ulva*. However, from second week on, second and third cultures experimented lower growth rates, having nutrient limitation caused by the addition of saltwater refilling instead of water from biofilter. **Fig.16** shows the SGR evolution of the three experiments:

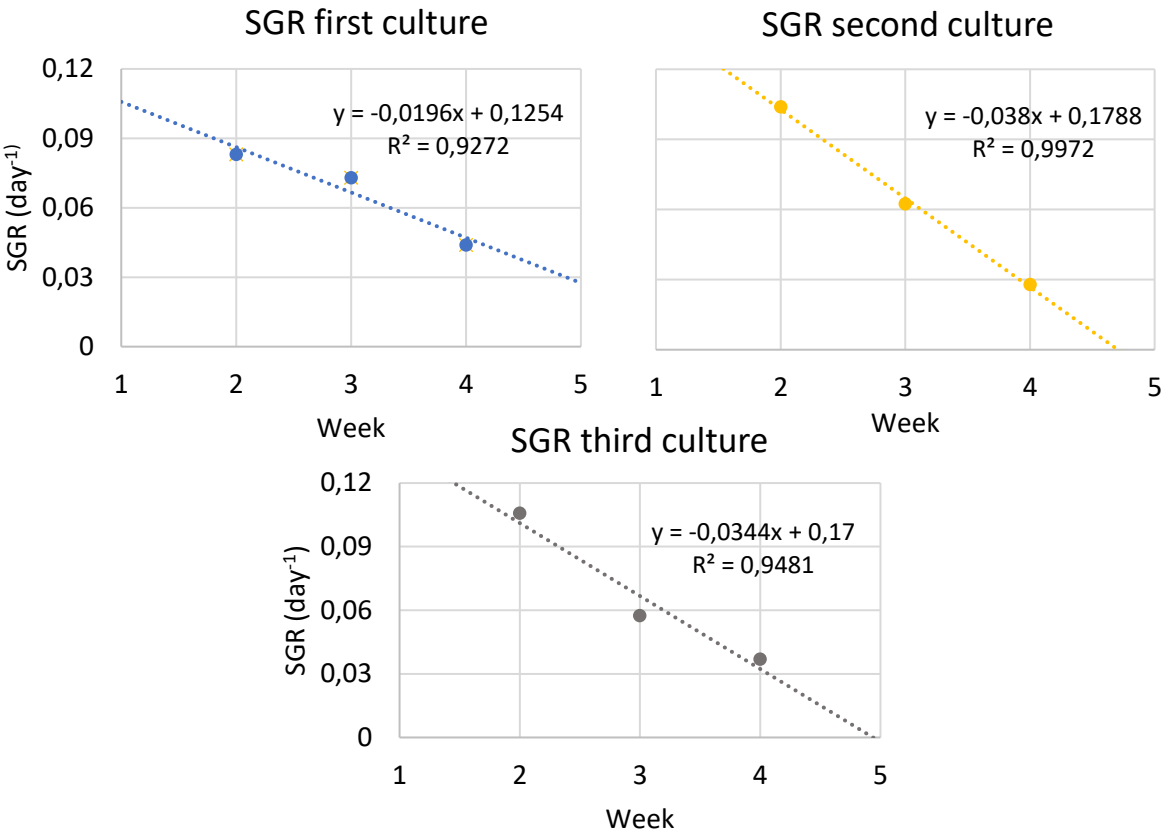

Fig 16: Fit functions and evolution of SGR for each culture

The lower decrease on SGR was in the first culture, in which there were no nutrient limitations. In addition, SGR on the second and third cultures followed a similar evolution, meaning that the amount of light (determined by LEDs distance of 10 and 6 cm) did not affect the algae growth as much as the nutrient limitation.

The way of mixing in our tubular PBR was air coming from the bottom of the cylinder. When the algae surface starts growing, little air bubbles are more easily stuck below the algae, impeding them to return to the bottom and finally piling them up on the surface. Such problems appeared when the total amount of biomass inside the tank reached approximately 20-25g (between weeks 3 and 4), or what is the same, an approximate culture density of 0.7 g/l.

Finally, the chlorophyll content did not vary during the course of the first and second culture. The starting algae was taken from tank R3 of IMTA, with a total chlorophyll content of 68.22 µmol m^{-2}, and no significative differences were determined. However, the final chlorophyll content during the third experiment decreased to 54.91 µmol m^{-2}, which can be explained by a light excess inside the photobioreactor.

4.2. Model performance

Before carrying out the proposed model, some parameters regarding the PBR geometry, light conditions and culture properties must be determined. Those parameters can be found either bibliographically (like the water extinction coefficient *Kw*) or experimentally (as seaweed extinction coefficient *Kx* or the PBR geometry).

Once those parameters are found, the model will be tested in different situations, simulating the light distribution inside the reactor varying the algae density, predicting the amount of biomass while measuring the light at the centre, and comparing the obtained results with the real ones.

4.2.1. Experimental *Kx*

The last unknown parameter needed for the model is *Kw* or seaweed light extinction coefficient. If we solve the **Eq. 3** and isolate *Kx* we obtain:

$$Kx = \frac{\frac{ln\frac{I(R,\theta)}{I_0(\theta)}}{-R} - GF(\theta) - Kw}{X} \quad \textbf{Eq. 10}$$

In order to obtain the most accurate value of *Kx*, some experiments were carried out varying the amount of biomass and measuring PAR at the centre. **Eq. 10** was implemented on the data of **Table 5**, varying the values of *I(R,θ)* and *X*, and obtaining a final value of *Kx* = 0.0166 $m^2\ g^{-1}$ with a standard deviation of 0.001 from the mean, which from now on, will be the chosen value for the seaweed light extinction coefficient.

4.2.2. I_0 performance

As it was explained in chapter **3.5.3**, our model takes numerical values for the Amplitude and the Centre of the sinusoidal function that represents the irradiance on the photobioreactor walls. However, taking experimental values of the PAR at the PBR surface we will be able to see how well the obtained values fit the sinusoidal function (**Eq.7**) and how close are the Model-values from the Excel's Solver-values. Having a pitch (distance between each LED's spiral) equal to 10 cm, we obtain the following results:

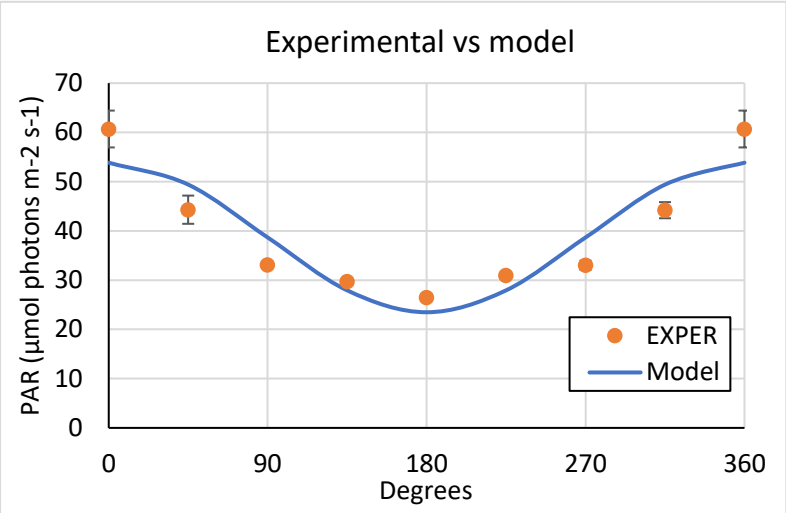

'Solver' values

A	15,18
B	38,66
R^2	**0,91**

Model values

A	20.2
B	43.5

Fig 17: On the left, Experimental PAR values fitted with 'Solver' (Excel) using **Eq.7**. On the right, A and B values from 'Solver' and Model approximation using Eq. (LEDs pitch = 10 cm)

Measuring PAR alongside the perimeter of any section of the PBR we get the last results, which show that the proposed sinusoidal function is very closed to the reality, obtaining a correlation coefficient (R^2) equal to 0.91. Althought the 'Solver' values obtained with Excel express the best values of A and B for **Eq.7**, values proposed by the model are also very closed to them, obtaining the same correlation coefficient as with the first ones.

Another test is carried out in order to prove the correct performance of our model. Now, having a picth (distance between LEDs spirals) of 6 cm, we obtained the following results:

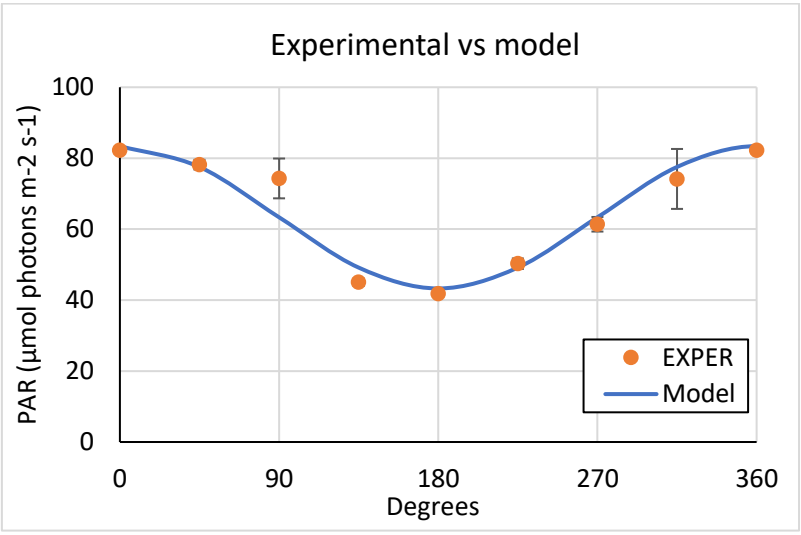

'Solver' values

A	20,06
B	63,35
R^2	**0,96**

Model values

A	20.2
B	62.0

Fig 18: On the left, Experimental PAR values fitted with 'Solver' (Excel) using **Eq.7**. On the right, A and B values from 'Solver' and Model approximation using Eq. (LEDs pitch = 6 cm)

Comparing last **Figure 17** with **Figure 18**, we can see how the values of Amplitude and Center determine the shape of the sinusoidal function that will take the model for the simulation of I_0 matrix.

4.2.3. Input Data

Finally, once the experimental value of the seaweed extinction coefficient '*Kx*' has been determined, and the correct performance of the function I_0 has been tested, we have to introduce the following data into the model description:

Table 4: Input data of the proposed model

	Value	**Units**	**Description**
PBR dimensions			
V	0.04	m^3	PBR volume
R	0.07	m	PBR radius
Light conditions	*(LEDs pitch) 10/6 cm*		
Imig	45/65	µmol m^{-2} s^{-1}	PAR without algae
I0deg	60/80	µmol m^{-2} s^{-1}	Highest PAR perimeter
I180degr	26/40	µmol m^{-2} s^{-1}	Lower PAR perimeter
Culture properties			
Kx	0.01655	m^2 g^{-1}	Algae coefficient
Kw	1.5	m^{-1}	Water coefficient
Measure of light			
Llum_int	*	µmol m^{-2} s^{-1}	PAR with algae

Once we have all the previous data, the model will be able to simulate light distribution. *Llum_int* will be the measure of light at the centre of the PBR when we do not know the amount of biomass. Taking such value as a starting point, the model will also approximate the amount of biomass inside the reactor taking into account the light extinction by means of Lambert-Beer's law.

4.2.4. Flowchart

The following diagram represents the steps followed by the program to simulate the light distribution and the biomass approximation. The symbology used is the following: a circle for start and ending, a rectangle for processes, and a rhomboid for input/output data.

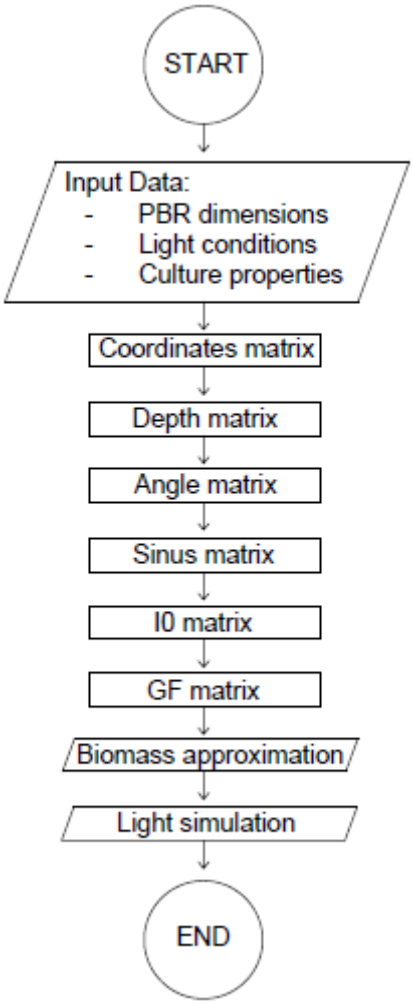

Fig 19: Flowchart for the proposed model

As we can see, the model obeys a linear methodology, in which every step depends on the previous one. Due to this linearity, there are no decisions to take, so the results returned by the program will be strongly related with the input data explained in chapter **4.2.3**.

4.2.5. Light distribution

In order to test how biomass affects the light distribution inside be PBR, two different experiments were carried out varying the distance between LEDs. PAR at the centre of the tank was measured within different algae densities, and the obtained value was introduced to the model. **Table 5** shows the results:

Table 5: PAR measurements at the centre of the PBR for each Biomass tested and their respective Standard Deviation (n=40)

		LEDs Pitch = 10 cm		**LEDs Pitch = 6 cm**	
Biomass (g)	**Density (g/l)**	PAR ($\mu mol\ m^{-2}\ s^{-1}$)	St. Dev.	PAR ($\mu mol\ m^{-2}\ s^{-1}$)	St. Dev.
15	3.75	30.59	3.37	40.61	3.34
20	5.00	25.01	3.34	32.78	3.31
25	6.25	20.87	2.04	31.95	4.62
30	7.50	18.36	1.68	27.61	3.60
35	8.75	15.19	1.59	19.23	2.70
40	10.00	15.15	2.24	20.12	2.27
45	11.25	12.64	1.64	16.95	2.61
50	12.50	10.10	2.20	14.71	3.35
55	13.75	9.58	2.06	12.75	3.12

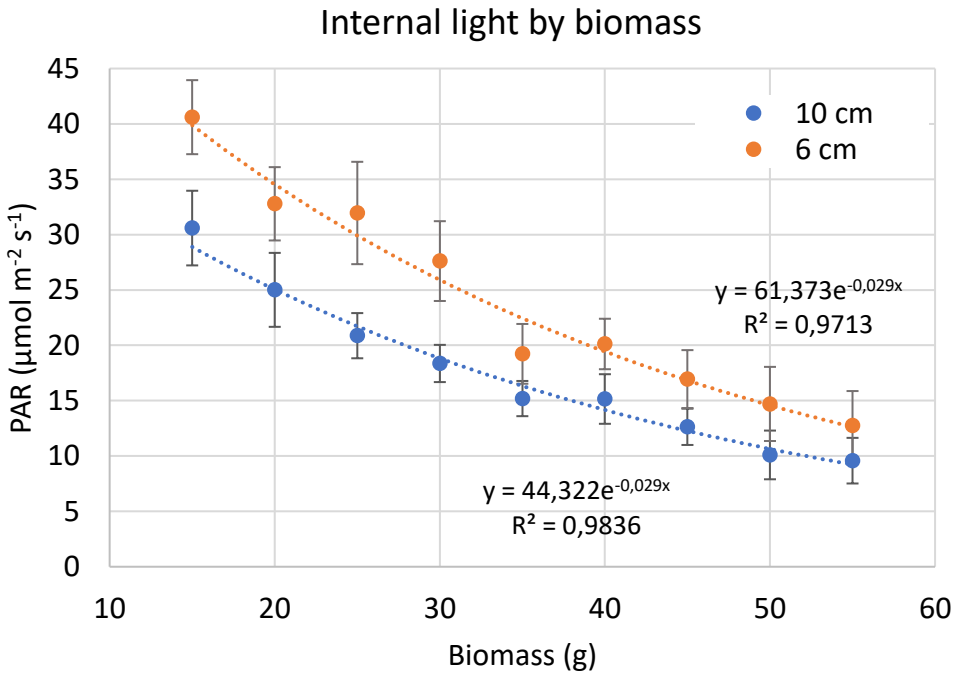

Fig 20: Fitting functions of PAR against Biomass of every LED disposition

As it is shown in **Fig.20**, having a shorter distance between LEDs makes the centre of the PBR more illuminated. Both configurations follow an exponential decrease with strong correlation coefficients.

The chosen amounts for these experiments were from 15g to 55g. As we are working with macro algae, light measurement relies on the culture homogeneity, so biomass under 15g would make the results non relevant and too scattered from a mean, with a very high standard deviation. Furthermore, the mixing method cannot work with amounts above 55g, so most of the algae get stuck on the water surface.

PAR data for every algae density summarized in **Table 5** was introduced to the model. The light distribution inside the tank is represented by a contour plot, which contains the PAR isolines in each point of a section. **Fig.22** in page 43 shows eight plots of the most representative light distributions regarding both experiments with 10 and 6 cm of distance between LEDs.

Having a shorter distance between LEDs makes the PBR section more illuminated. The reduction of the chlorophyll content during the third experiment, which decreased from 68.22 to 54.91 µmol m^{-2}, can be explained by an excess of light with the 6 cm configuration.

The last way of simulating light distribution is using three-dimensional surface plots, shown in **Fig.21**. Values of PAR are plotted as heights above the PBR section, representing the helicoidal LEDs shape and visualizing the exponential light extinction using Lambert-Beer law:

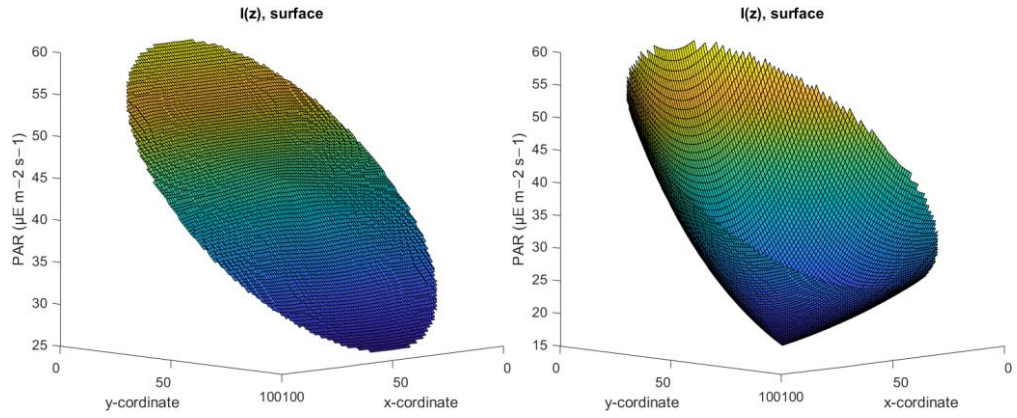

Fig 21: Three-dimensional plot of the PAR irradiance inside the PBR (figures a) 0g and b) 35g of *Ulva ohnoi* with 10 cm of LEDs distance)

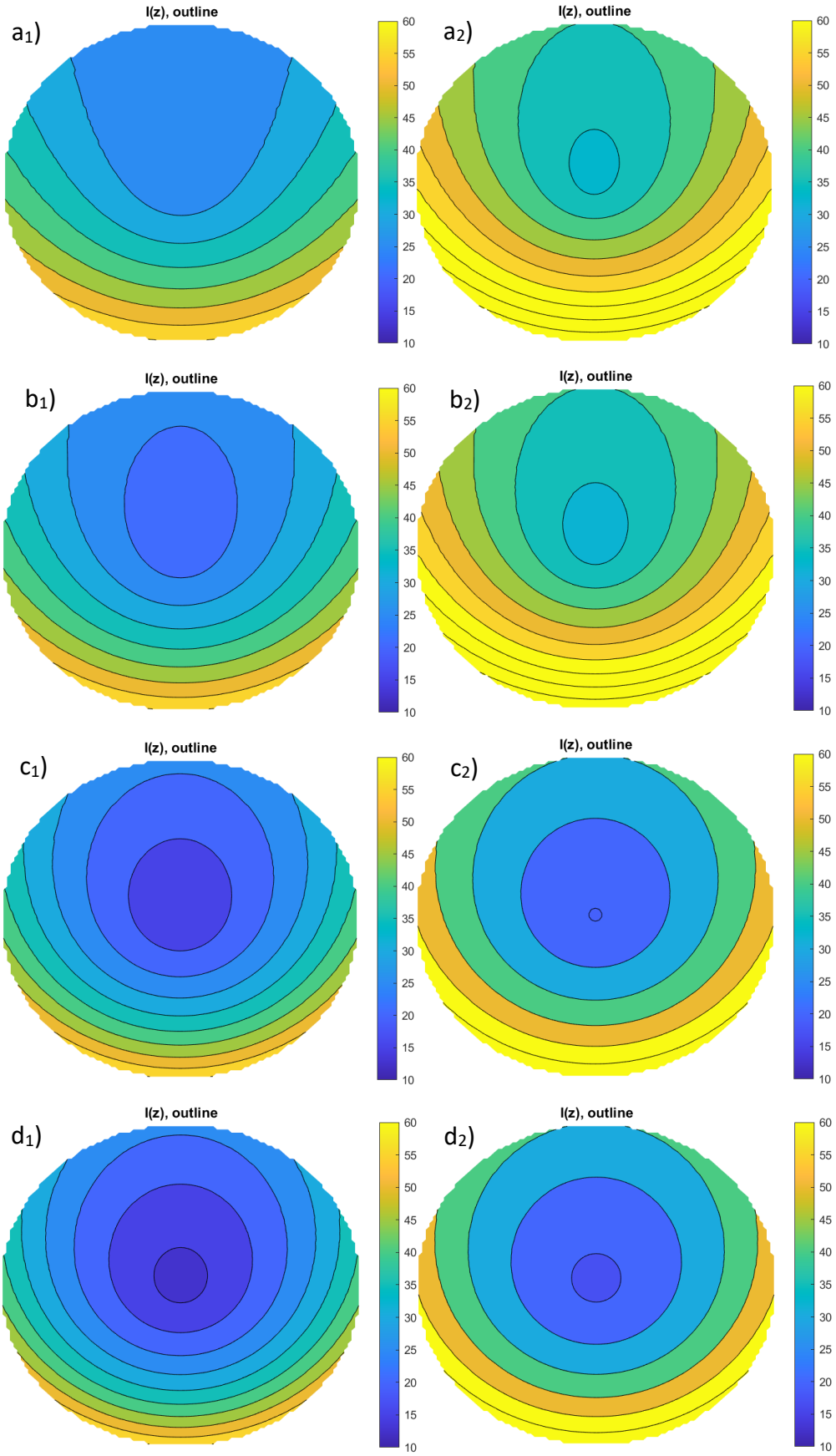

Fig 22: PBR light distribution for LED distance of 10 cm (first column) and 6cm (second column). Biomass = a) 20g, b) 25g, c) 35g and d) 45g

4.2.6. Biomass approximation

Finally, the model returns the value of the predicted amount of biomass inside the PBR regarding the value of the central PAR previously introduced. **Eq.11** shows how the model finds the biomass approximation: applies Lambert-Beer law described previously in **Eq.5** isolating the term of Biomass. Although we can apply **Eq.11** for any θ of the section, angle θ = 0º is by default implemented.

$$X = \frac{\frac{\ln\left(\frac{I(R,\theta)}{I0(\theta)}\right)}{-R} - GF(\theta) - Kw}{Kx} * V \qquad \textbf{Eq 11}$$

Table 6 shows the summarized data of the results obtained with the proposed model, and a correlation plot between the predicted and the real biomass is represented in **Fig.23**:

Table 6: On left, comparison between real biomass and the one predicted by the model and their respective correlation coefficient R^2

	Predicted Biomass (g)	
Real Biomass (g)	LEDs Distance 10 cm	LEDs Distance 6 cm
15	13,3	16,2
20	20,3	23,6
25	26,5	24,5
30	30,9	29,6
35	37,5	35,2
40	37,6	40,5
45	43,8	46,4
50	51,6	51,3
55	53,4	56,2
R^2	**0.9917**	**0.9959**

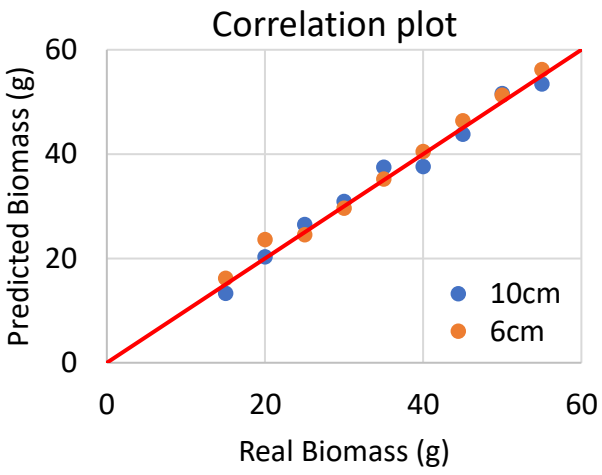

Fig 23: On right, correlation plot between real and predicted biomass

The high correlation observed between the measured PAR with both predicted and real *Ulva* biomass suggests that the model would be suitable for a fast biomass estimation in PBRs. The PBR limitations of volume and mixing method impede us to carry out samples higher than 55 g of biomass.

We can also ask Matlab to fit values between PAR at the centre and the real biomass for the LEDs distance of 10 cm, described previously in **Table 6.** In addition, we can add predictive bound at the 95% of confidence level, getting from the SSE (Sum of Squared estimate of Errors, in this case SSE = 20.67). Applying these commands, we get the following plot:

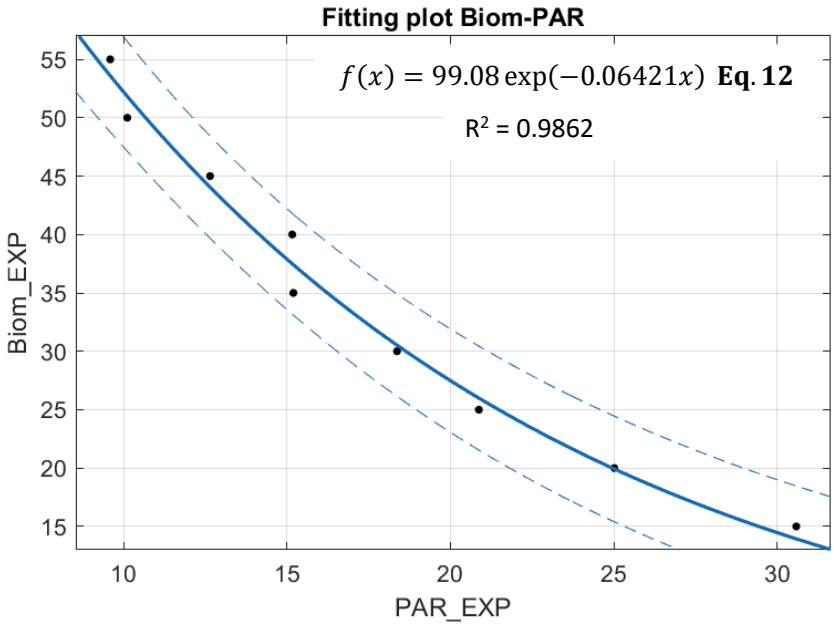

Fig 24: Fitting plot of Real Biomass against the value of PAR at the centre of the PBR (10 cm LEDs distance)

Predictive bounds shows the biomass intervals in which the PBR is working. As we are working with macro algae, higher PAR values mean more heterogeneity in the culture, having higher dispersion with lower biomass densities.

Finally, the fit function on **Fig.24** can be represented numerically, with **Eq.12.** If we take again the equation obtained from Lambert-Beer law, which we used to calculate the predicted amount of biomass (**Eq.11**), and compare with this **Eq.12**, we would see that they have a very strong correlation coefficient between them (R^2 = 0.991), which means that we have obtained the same from two different ways.

4.3. Comparison with Evers model

Results obtained using Evers model were not as good as the obtained with the proposed Lambert-Beer law. The first step was to adapt **Eq.3** explained in Chapter **1.4.3** to our conditions, applying *Kw* and *Kx* in spite of α. Geometric Factor GF(θ) was not applied for this model because it was determined directly isolating from Lambert-Beer law. **Eq.3** was transformed into **Eq.13**:

$$\boldsymbol{I(z,\theta,X) = \frac{1}{\pi}\int_0^{\pi} I(\theta,z,X)d\theta}$$

$$\boldsymbol{= \frac{I_0(\theta)}{\pi}\int_0^{\pi} \exp\{-(Kw + Kx * X) * \left[(R-z)\cos\theta + (R^2 - (R-z)^2 \sin^2\theta)^{0.5}\right]\}d\theta \quad Eq.13}$$

Then, applying the previous formula to and adaptation of our model, 'contourf' plots were represented, obtaining the following results:

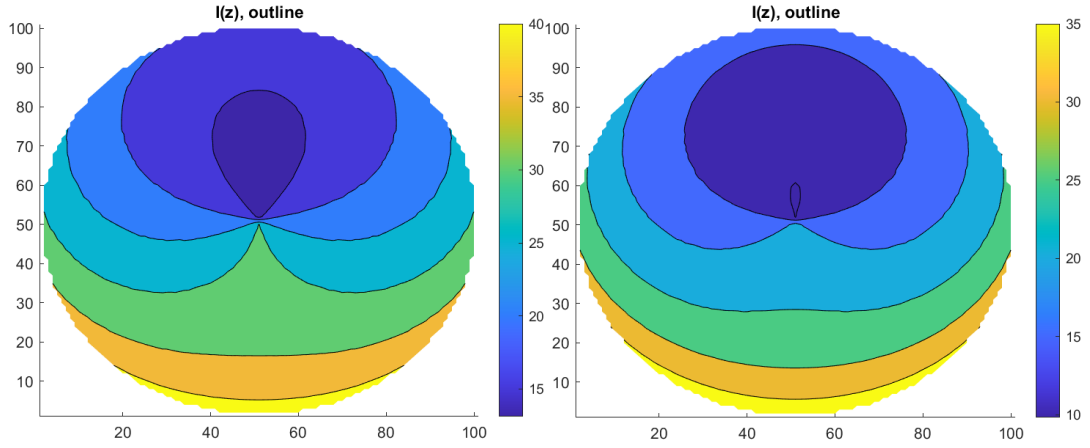

Fig 25: Contour plot using Evers model with 25 g of biomass on the left plot and 35 g on the right one and LED's pitch of 10 cm

Due to the complexity of the model, it was very difficult for us to isolate the biomass term from the equation, so values of **Table 6** could not be compared. There are many differences between Evers model and the one used previously: on the one hand, Evers considers that light follows a diffused flow, so light reaches one point coming from all directions. On the other hand, considering that light follows a direct flow, makes the proposed model easier to work with, obtaining a very good fit explained during the last chapters using Lambert-Beer law.

5. CONCLUSION

The research carried out during these months has allowed us to draw the following conclusions:

- In terms of the photobioreactor used, the proposed model has worked efficiently. The total biomass approximations were very closed to the real ones, even changing the LEDs shape, and the light distribution plots give us a clear vision of how light is attenuated inside the reactor. It can be said that the proposed model could be a very useful tool to work with, if its performance in other tubular reactors is as good as ours.
- *Ulva ohnoi* productivity was limited to the mixing methodology of the PBR, obtaining a maximum density of 0.7 g/l before algae start getting stuck on the surface.
- No visual differences in the algae growth were observed between 10 and 6 cm of distance between LEDs. Therefore, the second configuration would be enough for the correct culture growth, irradiating less light and consequently obtaining an energy saving.

6. BIBLIOGRAPHY

Acién Fernández, F. G., García Camacho, F., Sánchez Pérez, J. A., Fernández Sevilla, J. M., & Molina Grima, E. (1997). A model for light distribution and average solar irradiance inside outdoor tubular photobioreactors for the microalgal mass culture. *Biotechnology and Bioengineering*, *55*(5), 701–714. https://doi.org/10.1002/(SICI)1097-0290(19970905)55:5<701::AID-BIT1>3.0.CO;2-F

Azzopardi, B. (2019). *Asparagopsis taxiformis (Red Algae) - Atlantis Gozo*. 21/01. https://www.atlantisgozo.com/asparagopsis-taxiformis-red-algae/ (Consulted 14 March of 2021)

Barsanti, Laura & Gualtieri, P. (2010). *Algae: Anatomy, Biochemistry, and Biotechnology, Second Edition - Laura Barsanti, Paolo Gualtieri - Google Libros*. https://books.google.es/books?hl=es&lr=&id=AZClAgAAQBAJ&oi=fnd&pg=PP1&dq=red+algae+anatomy&ots=aG97Zj03xe&sig=s1dcFQ3o8anjH06Te3nhTvdPFNM#v=onepage&q=red algae anatomy&f=true (Consulted 14 March of 2021)

Baweja, P. (2016). *Ulvales - an overview (pdf) | ScienceDirect Topics*. https://www.sciencedirect.com/topics/agricultural-and-biological-sciences/ulvales/pdf (Consulted 14 March of 2021)

Beltrán-Rocha, J. C., Guajardo-Barbosa, C., Barceló-Quinta, I. D., & López-Chuken, U. J. (2017). Biotreatment of secondary municipal effluents using microalgae: Effect of pH, nutrients (C, N AND P) and CO2 enrichment. *Revista de Biologia Marina y Oceanografia*, *52*(3), 417–427. https://doi.org/10.4067/s0718-19572017000300001

Britannica, T. E. of E. (2018). *Brown algae | class of algae | Britannica*. 10/03. https://www.britannica.com/science/brown-algae (Consulted 14 March of 2021)

Chopin, T. (2013). AquacultureAquaculture, Integrated Multi-trophic (IMTA)aquacultureintegrated multi-trophic (IMTA). In P. Christou, R. Savin, B. A. Costa-Pierce, I. Misztal, & C. B. A. Whitelaw (Eds.), *Sustainable Food Production* (pp. 184–205). Springer New York. https://doi.org/10.1007/978-1-4614-5797-8_173

Ellis, J., & Tiller, R. (2019). Conceptualizing future scenarios of integrated multi-trophic aquaculture (IMTA) in the Norwegian salmon industry. *Marine Policy*, *104*(March), 198–209. https://doi.org/10.1016/j.marpol.2019.02.049

Erickson, L. E. (2011). Bioreactors for Commodity Products. In *Comprehensive Biotechnology, Second Edition* (Second Edi, Vol. 3). Elsevier B.V. https://doi.org/10.1016/B978-0-08-088504-9.00236-1

Evers, E. G. (1990). A Model. *Biotechnology and Bioengineering*, *38*(3), 254–259. https://doi.org/10.1002/bit.260380307

Grimes, S., Benabdi, M., Babali, N., Rrefes, W., Boudjellal-Kaidi, N., & Seridi, H. (2018). Mediterranean Marine Science. *Mediterranean Marine Science*, *19*(1), 156–179. https://ejournals.epublishing.ekt.gr/index.php/hcmr-med-mar-sc/article/view/13824/15226

Hiraoka, M., Shimada, S., Uenosono, M., & Masuda, M. (2004). A new green-tide-forming alga, Ulva ohnoi Hiraoka et Shimada sp. nov. (Ulvales, Ulvophyceae) from Japan. *Phycological Research*, *52*(1), 17–29. https://doi.org/10.1111/j.1440-1835.2004.tb00311.x

Katsuda, T., Arimoto, T., Igarashi, K., Azuma, M., Kato, J., Takakuwa, S., & Ooshima, H. (2000). Light intensity distribution in the externally illuminated cylindrical photo-bioreactor and its application to hydrogen production by Rhodobacter capsulatus. *Biochemical Engineering Journal*, *5*(2), 157–164. https://doi.org/10.1016/S1369-703X(00)00054-1

Krueger-Hadfield, S. A., Kollars, N. M., Byers, J. E., Greig, T. W., Hammann, M., Murray, D. C., Murren, C. J., Strand, A. E., Terada, R., Weinberger, F., & Sotka, E. E. (2016). Invasion of novel habitats uncouples haplo-diplontic life cycles. *Molecular Ecology*, *25*(16), 3801–3816. https://doi.org/10.1111/mec.13718

Lin, Q., & Lin, J. (2011). Effects of nitrogen source and concentration on biomass and oil production of a Scenedesmus rubescens like microalga. *Bioresource Technology*, *102*(2), 1615–1621. https://doi.org/10.1016/j.biortech.2010.09.008

Martinez, C. (2020). *El alga Kelp y sus beneficios para el organismo | Algamania*. 21/09. https://algamania.com/las-propiedades-del-alga-kelp/ (Consulted 14 March of 2021)

Masaló, I., & Oca, J. (2020). Evaluation of a portable chlorophyll optical meter to estimate chlorophyll concentration in the green seaweed Ulva ohnoi. *Journal of Applied Phycology*, *32*(6), 4171–4174. https://doi.org/10.1007/s10811-020-02257-3

Oca, J., Cremades, J., Jiménez, P., Pintado, J., & Masaló, I. (2019). Culture of the seaweed Ulva ohnoi integrated in a Solea senegalensis recirculating system: influence of light and biomass stocking density on macroalgae productivity. *Journal of Applied Phycology*, *31*(4), 2461–2467. https://doi.org/10.1007/s10811-019-01767-z

Patarra, R. F., Paiva, L., Neto, A. I., Lima, E., & Baptista, J. (2011). Nutritional value of selected macroalgae. *Journal of Applied Phycology*, *23*(2), 205–208. https://doi.org/10.1007/s10811-010-9556-0

Promdaen, S., Wattuya, P., & Sanevas, N. (2014). Automated microalgae image classification. *Procedia Computer Science*, *29*, 1981–1992. https://doi.org/10.1016/j.procs.2014.05.182

Rajendran, A. (2016). *Behavior of Light in a Photobioreactor and Design of Light Guides*. 4. http://openprairie.sdstate.edu/etd (Consulted 28 March of 2021)

Rosa, J., Lemos, M. F. L., Crespo, D., Nunes, M., Freitas, A., Ramos, F., Pardal, M. Â., & Leston, S. (2020). Integrated multitrophic aquaculture systems – Potential risks for food safety. *Trends in Food Science and Technology*, *96*(July 2019), 79–90. https://doi.org/10.1016/j.tifs.2019.12.008

Seo, Y. B., Lee, Y. W., Lee, C. H., & You, H. C. (2010). Red algae and their use in papermaking. *Bioresource Technology*, *101*(7), 2549–2553.

https://doi.org/10.1016/j.biortech.2009.11.088

Sevilla, J. M. F. (2014). *Importancia de la geometría y del modelo de transmisión*. Microalgal Biotechnology. https://w3.ual.es/~jfernand/ProcMicro70801207/index.html (Consulted 23 April of 2021)

Suh, I. S., & Lee, C. G. (2003). Photobioreactor engineering: Design and performance. *Biotechnology and Bioprocess Engineering*, *8*(6), 313–321. https://doi.org/10.1007/BF02949274

Waller, U., Buhmann, A. K., Ernst, A., Hanke, V., Kulakowski, A., Wecker, B., Orellana, J., & Papenbrock, J. (2015). Integrated multi-trophic aquaculture in a zero-exchange recirculation aquaculture system for marine fish and hydroponic halophyte production. *Aquaculture International*, *23*(6), 1473–1489. https://doi.org/10.1007/s10499-015-9898-3

Wichard, T., Charrier, B., Mineur, F., Bothwell, J. H., De Clerck, O., & Coates, J. C. (2015). The green seaweed Ulva: A model system to study morphogenesis. *Frontiers in Plant Science*, *6*(FEB), 1–8. https://doi.org/10.3389/fpls.2015.00072

7. APPENDIX

A. Nitrates determination in sea water

The following method is based on the UV absorption measure of the nitrate ion at 220nm. It is adequate as a screening method in not contaminated natural water samples. The absorption of the dissolved organic matter is corrected with the 275nm measure. The chloride ion does not affect the determination. The acid medium prevents the possible interference of the hydroxide or carbonate.

Apparatus

Spectrophotometer with UV lamp

10-50 mL syringes with membrane filters with 0.45µm of pores diameter

Volumetric flask of 50 mL

Pipettes of 1, 2, 5, 10, and 25 mL

Deionized water

Reagents

Nitrates stock solution of 100mg-1 $N\text{-}NO_3$. Dissolve 0.7218 g of KNO_3 (dried 1 hour in the stove) in a litre of deionized water.

Intermediate solution of 10 mg $N\text{-}NO_3$ L^{-1}. It is prepared by dilution 1/10 from the stock solution. It is frozen in 100 mL glasses

Chlorohydric acid 1M. 41.44 mL of concentrated HCl (37% and 1,19 g ml^{-1}) diluted until 500 mL with deionized water

Procedure

- Pattern of 0.2 mg of $N\text{-}NO_3$ L^{-1}. Pipette 1 mL of the intermediate solution of 10 mg $N\text{-}NO_3$ L^{-1} in a volumetric flask of 50 mL and fill in with deionized water until the mark.
- Pattern of 0.4 mg of $N\text{-}NO_3$ L^{-1}. Pipette 2 mL of the intermediate solution of 10 mg $N\text{-}NO_3$ L^{-1} in a volumetric flask of 50 mL and fill in with deionized water until the mark.
- Pattern of 0.8 mg of $N\text{-}NO_3$ L^{-1}. Pipette 4 mL of the intermediate solution of 10 mg $N\text{-}NO_3$ L^{-1} in a volumetric flask of 50 mL and fill in with deionized water until the mark.
- Pattern of 1 mg of $N\text{-}NO_3$ L^{-1}. Pipette 5 mL of the intermediate solution of 10 mg $N\text{-}NO_3$ L^{-1} in a volumetric flask of 50 mL and fill in with deionized water until the mark.
- Pattern of 2 mg of $N\text{-}NO_3$ L^{-1}. Pipette 10 mL of the intermediate solution of 10 mg $N\text{-}NO_3$ L^{-1} in a volumetric flask of 50 mL and fill in with deionized water until the mark.
- Pattern of 4 mg of $N\text{-}NO_3$ L^{-1}. Pipette 20 mL of the intermediate solution of 10 mg $N\text{-}NO_3$ L^{-1} in a volumetric flask of 50 mL and fill in with deionized water until the mark.

- Pattern of 5 mg of N-NO_3 L^{-1}. Pipette 25 mL of the intermediate solution of 10 mg N-NO_3 L^{-1} in a volumetric flask of 50 mL and fill in with deionized water until the mark.

Filter the sample with a membrane filter with pores diameter of 0.45 µm

Dilute if the predicted concentration is above to 5 mg N-NO_3 L^{-1}: pipette 2 mL of the sample in a volumetric flask of 50 mL and fill in until the mark

Add 1 mL of HCL to each pattern and sample

Lectures

Fix the wavelengths in the spectrophotometer: 220 nm and 275 nm

Adjust to zero the absorbance with deionized water (autozero bottom)

Read per duplicate the pattern values

Red per duplicate or triplicate the sample values

Obtain the equation and the R2 of the regression line taking:

x-axis: concentration values of 0, 0.2, 0.4, 0.8, 1, 2, 4, and 5 mg N-NO_3 L^{-1}.

y-axis: absorbance values obtained using the following equation:

Nitrate absorbance = lecture at ʎ(220nm) – 2 · lecture at ʎ(275nm)

Results

Fit the value of the calculated absorbance within the regression line and deduct the value of the concentration in mg N-NO_3 L^{-1}. If it has been done a dilution, apply the factor:

$$\frac{mg\ N-NO_3^-}{L\ dilution} * \frac{50\ mL\ dilution}{V\ mL\ sample} = \frac{mg\ N-NO_3^-}{L\ sample}$$

B. Determination of the soluble phosphorous in sea water

The following method determine the phosphate ions solved in sea water. It is a colorimetric method based on the reaction of heteropolyacid of phosphorous and molybdenum, which later it is reduced in the blue molybdenum compound (absorbance of 880nm).

Apparatus

Spectrophotometer with UV lamp

10-50 mL syringes with membrane filters with 0.45µm of pores diameter

Volumetric flask of 50 mL

Pipettes of 1, 2, 5, 10, and 25 mL

Deionized water

Reagents

Stock solution of 100 mg P L^{-1}: dissolve 0.4390 g of KH_2PO_4 (dried in a stove 1h at 105ºC) in 1 L of deionized water. We can keep it in the fridge.

Intermediate solution of 20 mg P L^{-1}: pipette 20 mL of the stock solution and fill in a volumetric flask of 100 mL until the mark with deionized water.

Reducer solution: solve 5 g of ascorbic acid ($C_6H_8O_6$) in 25 mL of deionized water and add 25 of sulphuric acid 4.5M. We can keep this solution on the fridge for over a week, until it gets a yellow colour.

Chromogen reagent: solve 12.5 g of tetrahydrate ammonium heptamolybdate ($((NH_4)6{\cdot}Mo_7O_{24}{\cdot}4H_20$) in 125 mL of water (solution 1). Dissolve 0.5 g of antimuonium and potassium tartrate ($K(SbO)C_4H_4O_6$) in 20 mL of water (solution 2). Finally, add to the first solution and then the second solution 350 ml of sulphuric acid 4.5M continuously waving.

Procedure

Prepare a solution of 5 mg P L^{-1}: pipette 25 ml of the intermediate solution (20 mg P L^{-1}) in a volumetric flask of 100 ml and fill in until the mark with deionized water.

- Pattern of 0.1 mg P L^{-1}: pipette 1 ml of the 5 mg P L^{-1} in a volumetric flask of 50 ml and fill in until the mark with deionized water.
- Pattern of 0.2 mg P L^{-1}: pipette 2 ml of the 5 mg P L^{-1} in a volumetric flask of 50 ml and fill in until the mark with deionized water.
- Pattern of 0.5 mg P L^{-1}: pipette 5 ml of the 5 mg P L^{-1} in a volumetric flask of 50 ml and fill in until the mark with deionized water.
- Pattern of 1 mg P L^{-1}: pipette 10 ml of the 5 mg P L^{-1} in a volumetric flask of 50 ml and fill in until the mark with deionized water.
- Blank: 50 ml deionized water

Filter the sample with a membrane filter with pores diameter of 0.45 µm

Dilute if the predicted concentration is above to 5 mg $N\text{-}NO_3$ L^{-1}: pipette 2 mL of the sample in a volumetric flask of 50 mL and fill in until the mark

Colour reaction

- Pipette 1 mL of the reducer solution in the solutions: blank, patterns and samples
- Shake
- Pipette 1 mL of the chromogen solution in the solutions: blank, patterns and samples
- Shake
- Wait 10 minutes

Lectures

Fix the spectrophotometer wavelengths at 880nm

Adjust the zero absorbance with blank solution

Read per duplicate the patterns values

Read per duplicate or triplicate the samples values

Obtain the equation and the R^2 of the regression line taking:

x-axis: concentration values of 0, 0.1, 0.2, 0.5 and 1 mg P L^{-1}.

y-axis: absorbance values for each pattern

Results

Fit the value of the calculated absorbance within the regression line and deduct the value of the concentration in mg P L^{-1}. If a dilution has been done, apply the corresponding factor.

C. Programming code – Matlab

```
%% LIGHT MODELLING IN A PHOTOBIOREACTOR
clear all
close all
%% INPUT DATA
% PBR dimensions
V = 0.04     ;          % Volume PBR (m3)
R = 0.07     ;          % Radius PBR (m)

% Light conditions
Imig = 45       ;       % PAR centre PBR without algae (µmol fotons m-2
s-1)
I0degr   = 60 ;         % PAR angle  = 0° (LED)
I180degr = 26 ;         % PAR angle  = 180° (middle LED's pitch)

% Culture properties
Kx = 0.01655 ;          % Coeficient extinció Ulva ohnoi (m2 gX-1),
experimental
Kw = 1.5     ;          % Coeficient extinció Aigua (m-1) (Oca-Masalo,
2019)

% Measure of light
Llum_int = 45;          % PAR centre PBR with unknown amount of algae
(µmol fotons m-2 s-1)
 % % % % % % % % % % %

%% DEFINICIÓ MATRIUS COORDENADES
x = (-50:50)' ;
y = (-50:50)  ;
X = zeros(101, 101);
Y = zeros(101, 101);
for i=1:101
    X(:,i) =  x(i);
    Y(i,:) = -y(i);
end

%% DEFINICIÓ MATRIU RADI
RADI = zeros(101, 101);
for i=1:101
    for j=1:101
        RADI(i,j) = (50 - sqrt(X(i,j)^2 + Y(i,j)^2))*R/50;
        if RADI(i,j) <= 0
                 RADI(i,j) = NaN;
        end
    end
end

%% DEFINICIÓ MATRIU ANGLE

Matrix = zeros(101, 101);
for i=1:101
    for j=1:101
        Matrix(i,j) = (X(51,101)*X(i,j)+Y(51,101)*X(i,j)) /
(sqrt(X(51,101)^2 + Y(51,101)^2) * sqrt(X(i,j)^2 + Y(i,j)^2))  ;

2- Establir dades del cercle --> Radi
    end
end
A = acosd(Matrix);
```

```
B = zeros(101,101);
for i=52:101
    for j=1:101
        B(i,j) = 360 - A(i,j);
    end
end
for i=1:101
    for j=1:101
        if i<=51
           A1(i,j) =  A(i,j);
        else
            A1(i,j) = A(i,j)*0;
        end
    end
end
ANGLE = round(B + A1);
for i=1:101
    for j=1:101
        if ANGLE(i,j) == 0
            ANGLE(i,j) = 360;
        end
    end
end
ANGLE(51,51) = 1;

%% DEFINICIÓ MATRIU SINUS

Ampl = (I0degr - I180degr)/2   ;    % Amplitud del sinus
Despl = Ampl + I180degr        ;    % Desplaçament en 'y' del sinus

SINUS = zeros(360, 2);
SINUS(1,1) = 1;
for i=2:360
    SINUS(i,1) = SINUS(i-1,1) + 1;
end
for i=1:360
    SINUS(i,2) = Despl + Ampl*sin(SINUS(i,1)*pi/180);
end

%% DEFINICIÓ MATRIU I0
for i=1:101
    for j=1:101
        I0(i,j) = SINUS(ANGLE(i,j),2);
    end
end

%% DEFINICIÓ MATRIU FG
for i=1:101
    for j=1:101
        FG(i,j) = log(Imig/I0(i,j))/-R-Kw;  %Factor Geometric
    end
end


%% CÀLCUL BIOMASSA
Biomassa = ((log(Llum_int / I0(51,51))/-R) - FG(51,51)-Kw)/(Kx);
Resultat_biomassa_aprox = Biomassa*V

%% DISTRIBUCIÓ LLUM
IZ = zeros(101,101);
```

```
for i=1:101
     for j=1:101
         IZ(i,j) = I0(i,j) * exp( - (FG(i,j) + Kw +
Kx*Biomassa)*RADI(i,j));
     end
 end

figure
hold on
surf(IZ)
title('I(z), surface')
xlabel('x-cordinate')
ylabel('y-cordinate')
zlabel('PAR (?E m?2 s?1)')
hold off

figure
hold on
contourf(IZ)
title('I(z), outline')
colorbar
caxis([10 60])
axis off

%% GRÀFICA DE CORRELACIÓ (adicional)
for i=1:40
    PAR(i) = i ;
    Biom(i) = ((log(PAR(i) / I0(51,52))/(-0.07)) - FG(51,52) -
Kw )/Kx*V;
end

Biom_EXP = [ 15, 20, 25, 30, 35, 40, 45, 50, 55 ];   %BIOMASSA
PAR_EXP  = [ 30.59, 25.015, 20.87, 18.365, 15.19, 15.155, 12.64,
10.105, 9.58 ]; %LLUM

figure
plot(PAR_EXP(:),Biom_EXP(:), 'o')
hold on
plot(PAR(:), Biom(:))
title('Fitting plot Biomass - PAR')
xlabel('PAR light (µmol fotons m-2 s-1) ')
ylabel('Biomass (g)')
legend('Experimental', 'Fit')
xlim([5 35])
hold off
```